

NUCLEOCYTOPLASMIC shuttling of ETHYLENE RESPONSE FACTOR 5 mediated by nitric oxide suppresses ethylene biosynthesis in apple fruit

Yinglin Ji¹ , Mingyang Xu¹, Zhi Liu², Hui Yuan¹ , Tianxing Lv², Hongjian Li^{1,2}, Yaxiu Xu¹, Yajing Si¹ and Aide Wang¹ 

¹Key Laboratory of Fruit Postharvest Biology (Liaoning Province), Key Laboratory of Protected Horticulture (Ministry of Education), National & Local Joint Engineering Research Center of Northern Horticultural Facilities Design & Application Technology (Liaoning), College of Horticulture, Shenyang Agricultural University, Shenyang 110866, China; ²Liaoning Institute of Pomology, Xiongyue 115009, China

Summary

Author for correspondence:
Aide Wang
Email: awang@syau.edu.cn

Received: 18 January 2022
Accepted: 28 February 2022

New Phytologist (2022) **234**: 1714–1734
doi: 10.1111/nph.18071

Key words: apple (*Malus domestica*), ethylene, ETHYLENE RESPONSE FACTOR 5 (ERF5), fruit ripening, nitric oxide (NO), nucleocytoplasmic shuttling.

- Nitric oxide (NO) is known to modulate the action of several phytohormones. This includes the gaseous hormone ethylene, but the molecular mechanisms underlying the effect of NO on ethylene biosynthesis are unclear.
- Here, we observed a decrease in endogenous NO abundance during apple (*Malus domestica*) fruit development and exogenous treatment of apple fruit with a NO donor suppressed ethylene production, suggesting that NO is a ripening suppressor.
- Expression of the transcription factor *MdERF5* was activated by NO donor treatment. NO induced the nucleocytoplasmic shuttling of *MdERF5* by modulating its interaction with the protein phosphatase, *MdPP2C57*. *MdPP2C57*-induced dephosphorylation of *MdERF5* at Ser260 is sufficient to promote nuclear export of *MdERF5*. As a consequence of this export, *MdERF5* proteins in the cytoplasm interacted with and suppressed the activity of *MdACO1*, an enzyme that converts 1-aminocyclopropane-1-carboxylic acid (ACC) to ethylene. The NO-activated *MdERF5* was observed to increase in abundance in the nucleus and bind to the promoter of the ACC synthase gene *MdACS1* and directly suppress its transcription.
- Together, these results suggest that NO-activated nucleocytoplasmic *MdERF5* suppresses the action of ethylene biosynthetic genes, thereby suppressing ethylene biosynthesis and limiting fruit ripening.

Introduction

Nitric oxide (NO) is a free radical, reactive gaseous molecule with a broad spectrum of regulatory functions in plant growth and development (Besson-Bard *et al.*, 2008), including seed germination (Beligni & Lamattina, 2000), root development (Correa-Aragunde *et al.*, 2004; Yu *et al.*, 2014), flowering (He *et al.*, 2004), reproduction (Prado *et al.*, 2004), fruit ripening, senescence (Ya'acov *et al.*, 1998), and responses to biotic and abiotic stresses (Besson-Bard *et al.*, 2008). The multiple fundamental roles of NO have been highlighted through the characterization of mutants of *Arabidopsis* (*Arabidopsis thaliana*) that are impaired in NO production or turnover, and some that show severe pleiotropic phenotypes (He *et al.*, 2004; Feechan *et al.*, 2005; Lee *et al.*, 2008). A major research focus has been on NO involvement in the modulation of the action of plant hormones, such as auxin (Otvos *et al.*, 2005), cytokinin (Wilhelmova *et al.*, 2006), abscisic acid (ABA; Bodanapu *et al.*, 2016) and ethylene (Bowyer *et al.*, 2003; Duan *et al.*, 2007; Kolbert *et al.*, 2019; Fenn & Giovannoni, 2021). Ethylene is regarded as the key

hormone that regulates the ripening of climacteric fruit (Fenn & Giovannoni, 2021), but the detailed molecular mechanism by which NO affects ethylene biosynthesis is still unclear.

Early studies suggested the endogenous production of NO has a regulatory effect on the maturation of commercial produce (Ya'acov & Haramaty, 1996). Subsequently, it was found that endogenous NO production in some immature fruits was significantly higher than in mature fruits, whereas ethylene production shows the opposite pattern (Leshem & Wills, 1998). For example, endogenous NO production in immature banana (*Musa acuminata*) fruit was observed to be approximately four-fold higher than in the mature fruit (Leshem & Wills, 1998), whereas ethylene production was much lower in young banana fruit and gradually increased during the ripening process (Xiao *et al.*, 2013). Such studies suggested that NO may act as a natural growth regulator that can delay fruit ripening, and that its mechanism of action is associated with the inhibition of ethylene biosynthesis. Other studies of the ripening of various other fruits have consistently suggested that the primary mechanism of action of reactive

nitrogen species involves inhibition of the ethylene biosynthetic pathway (Rudell & Mattheis, 2006).

NO regulates a plethora of transcription factors via different mechanisms in plant cells. For example, NO induces the degradation of ABA-Insensitive 5 (ABI5) protein to promote seed germination and seedling growth (Albertos *et al.*, 2015). NO accumulation promotes zinc finger protein *S-nitrosothiol Regulated 1* (SRG1) and SRG3 expression, and triggers the *S*-nitrosylation of SRG1 and SRG3 to regulate plant immunity through different mechanisms (Cui *et al.*, 2018, 2021). Moreover, NO widely distributed in plants has been reported to influence the distribution of protein. For example, NO activated the transcription factor NONEXPRESSOR OF PATHOGENESIS-RELATED GENES1 (NPR1) oligomerization to prevent NPR1 from entering the nucleus (Tada *et al.*, 2008). However, the crosstalk between the NO and ethylene signaling pathway in ripening fruit has not been well-characterized.

In the ethylene cascade, SAM (*S*-adenosyl methionine) is formed from methionine (MT) by methionine adenosyl transferase (MAT), then SAM is converted into 1-aminocyclopropane-1-carboxylic acid (ACC) by ACC synthase (ACS) and further oxidized into ethylene by ACC oxidase (ACO) (Yang & Hoffman, 1984). Previous studies have demonstrated that ACS and ACO are the key rate-limiting enzymes in ethylene biosynthesis. For example, silencing of ACS or ACO in apple or tomato (*Solanum lycopersicum*) fruit reduces or prevents ethylene production (Dandekar *et al.*, 2004; Schaffer *et al.*, 2007; Gupta *et al.*, 2013). In this pathway, NO signals have been found to post-translationally modify MAT activity via *S*-nitrosylation to inhibit SAM turnover (Lindermayr *et al.*, 2006). Furthermore, the formation of a stable ternary ACC–ACO–NO complex (Rudell & Mattheis, 2006) and the reduction of ACC to 1-malonyl aminocyclopropane 1-carboxylic acid (MACC) have been shown to reduce ethylene formation (Zhu *et al.*, 2006). In addition, NO represses the expression of ACS and ACO, which results in reduced ethylene biosynthesis. For example, NO was found to delay the expression of ACO in tomato (Eum *et al.*, 2008) and banana (Cheng *et al.*, 2009). Moreover, transcript levels of *SIACS2* in tobacco (*Nicotiana (N.) benthamiana*) were found to be related to the concentration of applied NO (Ederli *et al.*, 2006).

During the signal transduction process, ethylene is perceived by receptors and the signal is transmitted to downstream positive responders ETHYLENE INSENSITIVE 2 (EIN2) and members of the EIN3/EIL (EIN3 like) family after a series of cascade reactions. In this pathway, EIN3/EIL is the core, or primary, transcription factor (TF) and it induces the secondary TF, ETHYLENE RESPONSE FACTOR (ERF), which in turn regulates the expression of downstream ethylene responsive genes (Lin *et al.*, 2009). However, little is known about whether crosstalk exists between the NO and ethylene signal transduction networks.

To date, studies to characterize the relationship between NO and ethylene biosynthesis have provided insights into the associated biochemical events (Corpas *et al.*, 2020), but the underlying genetic regulatory factors have yet to be resolved. We show here

that in apple fruit NO-activated MdERF5 functions as a nucleocytoplasmic signaling mediator by shuttling between the nucleus and cytoplasm, thereby suppressing the activity of ethylene biosynthetic genes and inhibiting ethylene production.

Materials and Methods

Plant materials and treatments

Apple (*Malus (M.) domestica* cv golden delicious (GD)) fruit were obtained from mature trees growing at the experimental farm of the Liaoning Pomology Institute (Xiongyue, China). Golden delicious fruit were harvested on the day of commercial harvest (145 d after full bloom, DAFB) when the content of total soluble solids reached 12% and immediately transferred to the laboratory. For an *in vivo* nitric oxide (NO) donor, sodium nitroprusside (SNP) treatment, fruit were immersed in 50, 100 or 200 μ M SNP (BBI Life Sciences, Shanghai, China) for 2 h. For another *in vivo* NO donor, *S*-nitrosoglutathione (GSNO) (Mur *et al.*, 2013) treatment, fruit were immersed in 50, 100 or 200 μ M GSNO (Sigma-Aldrich) for 2 h. Fruit were immersed in water for 2 h as a control. The fruit then were stored at room temperature (24°C) for 20 d, with sampling every 5 d during the storage period. In addition, GD fruit were harvested on the 130 DAFB were treated with NO-scavenger 2-(4-carboxyphenyl)-4,4,5,5-tetramethylimidazoline-1-oxyl-3-oxide (cPTIO; Sigma-Aldrich). For cPTIO treatment, the fruit were immersed in 200 μ M for 2 h and as a control, fruit were immersed in water for 2 h. All of the fruit then were stored at room temperature for 25 d and sampled every 5 d. At each sampling time, nine fruit were collected at random and divided into three groups (three fruit per group), giving three biological replicates. Fruit firmness and ethylene production were measured at each sampling time as described previously (Li *et al.*, 2014), at least three biological replicates were analyzed. Statistical significance was determined using a Student's *t*-test (**, $P < 0.01$).

Apple fruit calli (cv Orin) and *Nicotiana benthamiana* plants used for *Agrobacterium (A.) tumefaciens* infection were grown as described previously (Li *et al.*, 2016). For GSNO treatment of calli, 1 mM GSNO was added to the liquid Murashige & Skoog medium.

Gene expression analysis

Total RNA extraction, cDNA synthesis and quantitative real time (qRT)-PCR were conducted as described previously (Li *et al.*, 2015). RNA extracted from each pool of flesh (as described above) was used as one biological replicate, and a total of three biological replicates were analyzed. qRT-PCR was performed using a qTOWER³ G PCR System (Analytik Jena, Jena, Germany). Specific primers (Supporting Information Table S1) for each gene were designed using PRIMER3 (<http://frodo.wi.mit.edu>). The *MdActin* gene was used as internal control. Standard PCR was performed according to the method of Li *et al.* (2017).

Subcellular localization

The 1-aminocyclopropane-1-carboxylic acid (ACC) oxidase (MdACO1), ETHYLENE RESPONSE FACTOR (MdERF5) or protein phosphatase MdPP2C57 coding regions without the stop codon were cloned into the *EcoRI* and *KpnI* sites upstream of green fluorescent protein (GFP) in the pCambia1300 vector (BioVector, <http://www.biovector.net>) under their native promoter to form the ProMdACO1::MdACO1-GFP, ProMdERF5::MdERF5-GFP and ProPP2C57::MdPP2C57-GFP constructs. The constructs were co-infiltrated into *N. benthamiana* leaves with the mCherry-labeled marker NF-YA4-mCherry or PM-mCherry (Zhang *et al.*, 2019) using *A. tumefaciens*-mediated infiltration. The *N. benthamiana* plants were kept in the dark for 48 h post-infiltration. GSNO (100 μ M) then was injected into the infiltrated *N. benthamiana* leaves and imaging was performed 0, 2 and 12 h after GSNO treatment. GFP fluorescence was observed under a confocal microscope (TCS SP8; Leica, Wetzlar, Germany). For green fluorescence observation, the excitation wavelength was 488 nm and the emission wavelengths were 520–540 nm; for red fluorescence observation, the excitation wavelength was 561 nm and the emission wavelengths were 610–630 nm. The confocal microscope setting was kept identical when comparing nuclear/cytoplasmic signals. ProMdACO1::GFP, ProMdERF5::GFP or ProPP2C57::GFP were used as a control, respectively.

The protoplasts of maize (*Zea mays*) leaves were prepared as described previously (Yoo *et al.*, 2007). The phosphorylation-deficient and phosphomimetic forms of ProMdERF5::MdERF5-GFP were created by introducing mutations of Ser260 to either Ala (S260A) or Asp (S260D) using fast mutagenesis system (Transgen Biotech, Beijing, China; <http://www.transgen.com.cn>). All transient expression assays were repeated at least three times and representative results are shown.

Protein expression and purification

The full length MdACO1 sequence was inserted into the pEASY-E1 vector (Transgen Biotech) to express His fusion protein. The full-length MdERF5 sequence was inserted into the pGEX4T-1 vector (GE Healthcare, Chicago, IL, USA) downstream from GST. The resulting plasmids were transformed into *Escherichia coli* BL21 (DE3) competent cells. Recombinant fusion proteins were purified as described in Li *et al.* (2016).

Phosphatase assay

For the *in vitro* phosphatase assay, the *MdERF5* CDS was cloned into the *BamHI* and *SacI* sites downstream from the 3xFlag sequence under the control of the *CaMV 35S* promoter in the pRI101 vector (TaKaRa Bio, Kyoto, Japan). The recombinant *Pro35S::MdERF5-3xFlag* construct was infiltrated into *N. benthamiana* leaves using *A. tumefaciens* infiltration as described previously (Li *et al.*, 2017). Proteins extracted from the infiltrated *N. benthamiana* leaves were used for *in vitro* phosphatase analysis. A ProteinIso[®] Protein G Resin (Transgen Biotech) was used to

immunoprecipitate MdERF5-3xFlag using 10 μ l of anti-Flag antibody (1 mg ml⁻¹; TaKaRa Bio). The *MdPP2C57* CDS was inserted into the pGEX4T-1 vector downstream from glutathione S-transferase (GST). The resulting plasmid was transformed into *E. coli* BL21 (DE3) competent cells. Recombinant fusion proteins were purified as described above. The *in vitro* phosphatase assay was performed based on Umezawa *et al.* (2009) with modifications. MdERF5-3xFlag protein was immunoprecipitated from tobacco and mixed with 5 μ g of purified MdPP2C57-GST in phosphatase reaction buffer containing 20 mM HEPES (pH 7.5; Solarbio, Beijing, China), 20 mM MgCl₂ and 150 mM NaCl. Purified GST protein with a MdERF5-3xFlag was used as a negative control. The reaction was stopped after 30 min at 37°C by adding SDS-loading buffer. The reaction products were analyzed using the phos binding reagent acrylamide kit (APEX BIO Biotech, <https://www.apexbt.com/>).

For the *in vivo* phosphatase assay, the *MdPP2C57* CDS was cloned into the *KpnI* and *EcoRI* restriction sites downstream of the *CaMV 35S* promoter in the pRI101 vector. The recombinant *Pro35S::MdERF5-3xFlag* and *Pro35S::MdPP2C57* constructs were infiltrated into *N. benthamiana* leaves using *A. tumefaciens* infiltration as described previously (Li *et al.*, 2017). MdERF5-3xFlag was immunoprecipitated from tobacco leaf protein extracts and mixed with SDS-loading buffer. The reaction products were analyzed as described above.

Pull-down assay

In order to confirm the MdERF5-MdACO1 interaction, 5 μ g of purified recombinant GST-tagged MdERF5 (MdERF5-GST) was bound to protein Iso GST binding resin (Transgen Biotech). Recombinant poly-histidine-tagged MdACO1 (MdACO1-His) was added and samples incubated for 1 h at 4°C before immunoblot analysis as described previously (Li *et al.*, 2017). GST protein was used as the negative control.

Bimolecular fluorescence complementation (BiFC) assay

The *MdPP2C57* and *MdACO1* CDS were ligated into the pSPYNE-35S vector (Walter *et al.*, 2004) using the *BamHI* and *KpnI* sites. The *MdERF5* CDS was ligated into the pSPYCE-35S vector using the *BamHI* and *KpnI* sites. The resulting plasmids were introduced into *A. tumefaciens* strain EHA105, and then infiltration of *N. benthamiana* leaves was performed. All *N. benthamiana* were kept in the dark for 48 h, then GSNO (100 μ M) was injected into the infiltrated *N. benthamiana* leaves. The *N. benthamiana* leaves were visualized at 4 h after GSNO treatment. Yellow fluorescent protein (YFP) fluorescence was observed under a confocal laser scanning microscope (TCS SP8; Leica). For observation of yellow fluorescence, the excitation wavelength was 488 nm and the emission wavelengths were 520–540 nm; for red fluorescence observation, the excitation wavelength was 561 nm and the emission wavelengths were 610–630 nm. Fragments of MdERF5C and MdACO1 or MdERF5C and MdPP2C57 were used as negative controls. All transient

expression assays were repeated at least three times and the representative results were shown.

Yeast one-hybrid (Y1H) assay

Each fragment (*MdERF5*, *MdERF5N*, *MdERF5D*, *MdERF5D*) was ligated into the pGADT7 vector (TaKaRa Bio) using the *NdeI* and *EcoRI* restriction sites. The full-length *MdACS1* promoter was cloned into the pAbAi vector (TaKaRa Bio) using the *KpnI* and *XbaI* restriction sites (ACS, ACC synthase). All primers used are listed in Table S1. Transcription factor (TF) binding to the promoters was assayed using the Matchmaker™ Gold Y1H Library Screening System kit (cat. no. 630 491; TaKaRa Bio).

Electrophoretic mobility shift assay (EMSA)

For the EMSA, recombinant GST-tagged *MdERF5*, His-tagged *MdACO1* or GST-tagged *MdPP2C57* was expressed in *E. coli* BL21 (DE3) cells and purified as described above. The biotin-labeled *MdACS1* promoter regions contained a dehydration-related element (DRE) motif as shown in Fig. 8(b). Corresponding unlabeled regions were used as competitors. The EMSA analysis was completed as described previously (Li *et al.*, 2016).

Chromatin immunoprecipitation (ChIP)-PCR analysis

The *MdERF5* CDS was cloned into the *KpnI* and *EcoRI* sites downstream of the GFP sequence under the control of the CaMV 35S promoter in the pRI101 vector. The resulting *Pro35S::GFP-MdERF5* construct was transformed into apple calli, and ChIP assays were performed as described previously (Ji *et al.*, 2021) with an anti-GFP antibody. The amount of immunoprecipitated chromatin was determined by qPCR as described previously (Ji *et al.*, 2021). Each ChIP assay was repeated three times and the enriched DNA from each assay was pooled to one biological replicate for qPCR. At least three biological replicates were analyzed and a Student's *t*-test was employed to determine the statistical significance. Primers used are listed in Table S1.

RNA-seq of apple fruit

Control and GSNO-treated apple fruit sampled on Day 10 (stored at room temperature for 10 d post-harvest) were used for RNA-seq analysis. RNA extracted from control or GSNO-treated fruits (three biological replicates for each) were used for library construction and a total of six libraries were constructed. cDNA synthesis and library construction were performed as described previously (Huang *et al.*, 2014). RNA-seq was performed using an Illumina HiSeq2500 by Biomarker (<http://www.biomarker.com.cn/>). The fragments per kb per million reads (FPKM) method was used to calculate the rate of differential expressed genes. The false-discovery rate (FDR) with < 0.01 was used to determine the *P*-value thresholds via multiple testing. All genes selected had a fold-change ≥ 2.5 and a *P* < 0.05. The Unique gene identifier (Gene ID), log₂FC, FDR and

annotations are indicated in Table S2. All of the raw data has been deposited into the NCBI Sequence Read Archive under accession no. PRJNA658005. Other experimental methods are listed in Methods S1–S7.

Results

NO acts a suppressor of ethylene biosynthesis

In order to investigate the effect of NO on ethylene biosynthesis we chose the GD apple (*M. domestica*) cultivar, which produces a classical climacteric fruit with a rapid increase in ethylene production at the onset of ripening, as an experimental subject. We first measured the endogenous NO content of the fruit during development. Fruit were harvested every 30 d from 30 to 145 DAFB, where 145 DAFB is the day of commercial harvest. We observed that endogenous NO concentrations gradually decreased during fruit development (Fig. 1a). The changes of endogenous NO showed opposite trend with ethylene production which is increased gradually during GD fruit development (Li *et al.*, 2015), indicating a negative correlation between the production of nitric oxide and ethylene.

Next, GD apple fruit were harvested at 145 DAFB, treated with a NO donor, and stored at room temperature for 20 d (a period within which apple fruit complete ripening), after which fruit were sampled every 5 d. In 2017, apples harvested at the commercial harvest stage were treated with different concentrations of NO donor, GSNO (50, 100 and 200 μ M) or SNP (50, 100 and 200 μ M). All of the treatments significantly inhibited ethylene production, maintained fruit firmness and caused an increase in NO production compared with untreated control fruit during the storage period (Fig. S1a–f). We observed that the 100 μ M GSNO treatment had the largest effect on ethylene production (Fig. S1a–f) and so this concentration was used in the subsequent experiments. In 2018 and 2019, fruit harvested at the commercial harvest stage were treated with 100 μ M GSNO and we observed the same effect on ethylene production, NO production and fruit firmness as in 2017 (Figs 1b–e, S2a–d). In addition, the cPTIO treatment significantly promoted ethylene production and inhibited NO production compared with untreated control fruit during the storage period (Fig. 1f–h). These results further indicated that endogenous NO is a suppressor of ethylene biosynthesis.

NO activates the expression of *MdERF5*

We next investigated the expression of *MdACS1* and *MdACO1*, which are essential for ethylene biosynthesis in apple fruit (Dandekar *et al.*, 2004; Schaffer *et al.*, 2007). We observed that the expression of both genes was reduced after GSNO treatment (Figs 2a,b, S2e,f), suggesting that they are transcriptionally regulated by NO.

In order to elucidate the molecular mechanism by which NO regulates the ethylene biosynthetic genes, we compared the transcriptomes of apple fruit that were stored at room temperature for 10 d and treated, or not, with GSNO, using RNA sequencing

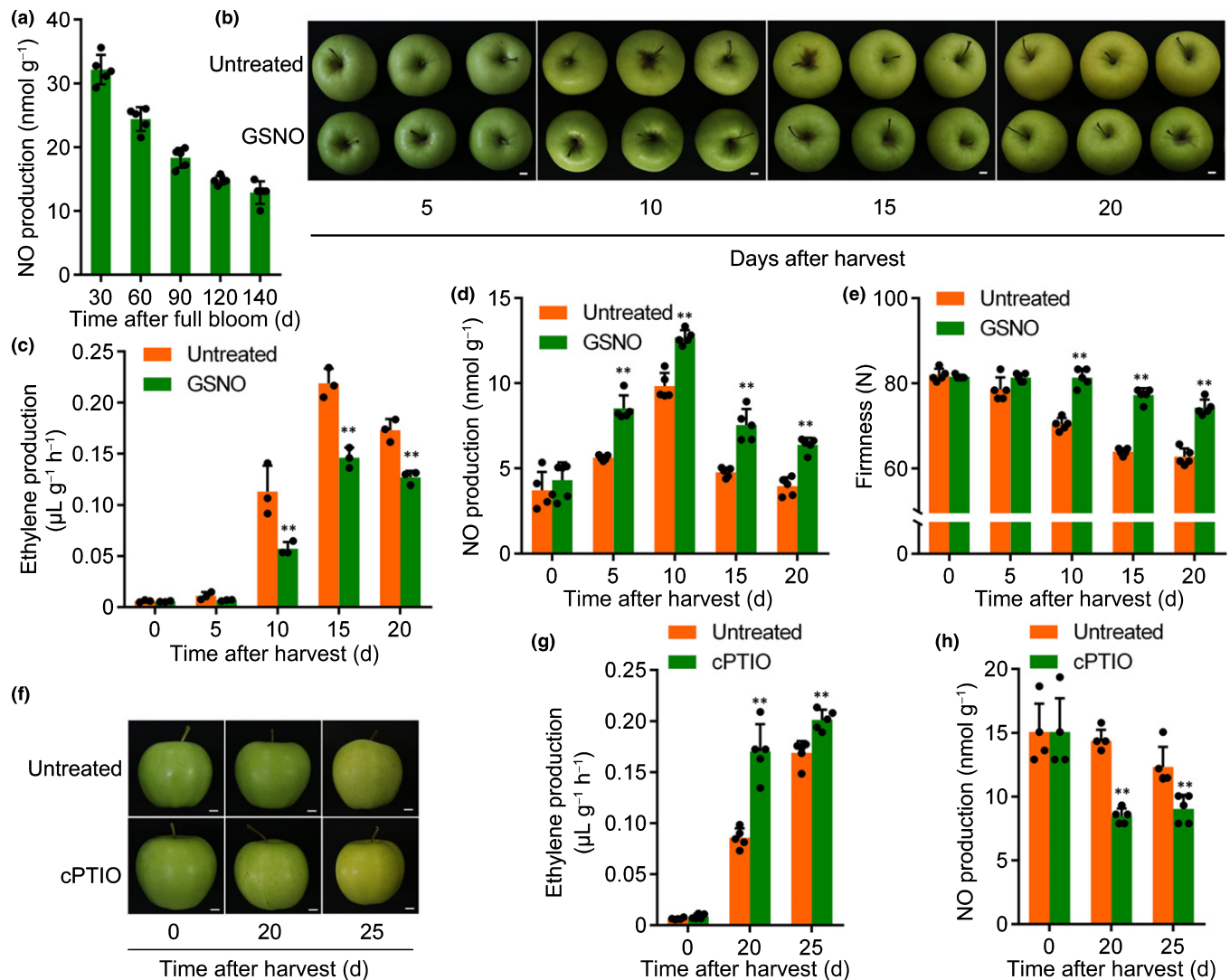


Fig. 1 Nitric oxide (NO) suppresses ethylene biosynthesis in apple fruit. (a) Endogenous NO content during apple fruit development in 2019. (b–e) Fruit collected on the day of commercial harvest (145 DAFB, d after full bloom) were treated with S-nitrosoglutathione (GSNO) and stored at room temperature for 20 d. After treatment, ethylene production (c), endogenous NO content (d), and fruit firmness (e) were measured. (f–h) Fruit collected at 130 DAFB were treated with the NO-scavenger 2-(4-carboxyphenyl)-4,4,5,5-tetramethyl-imidazole-1-oxyl-3-oxide (cPTIO) and stored at room temperature for 25 d. After treatment, ethylene production (g) and endogenous NO content (h). Bar, 1 cm. Untreated, fruit not receiving any treatment; GSNO, fruit treated with GSNO; cPTIO, fruit treated with cPTIO. Numbers under the x-axes of (c–e, g, h) indicate the storage duration (d) at room temperature after harvest; 0 indicates the day of harvest. Values represent means \pm SE. Each dot represents a biologically independent sample. Statistical significance was determined using a Student's *t*-test (**, $P < 0.01$).

(RNA-seq) (Table S2). Recent studies have shown that NO can affect protein phosphorylation in plants and mammals (Fan *et al.*, 2014), and we searched the RNA-seq data for genes encoding proteins with putative phosphorylation sites that showed a ≥ 2.5 -fold difference in expression between with GSNO-treated and untreated fruit. Only one *ERF* gene showed upregulated expression in GSNO-treated fruit compared to the control fruit (Table S3), and was found to be homologous to *AtERF6* which has been shown to be phosphorylated (Meng *et al.*, 2013). We cloned this gene from GD apple and named it *MdERF5*. We found that GSNO treatment promoted *MdERF5* expression during storage (Figs 2c, S3a,b) and that the expression of *MdERF5* gradually decreased during fruit development (Fig. S3c). In

addition, we observed that the expression of both *MdACS1* and *MdACO1* was activated and the expression of *MdERF5* was reduced after cPTIO treatment (Fig. 2d–f),

In order to address the importance of *MdERF5* in ethylene biosynthesis, we silenced its expression in apple fruit calli using *Agrobacterium*-mediated transformation. Six transgenic lines were generated, of which lines #1, #2 and #3 showed substantially reduced *MdERF5* transcript and protein levels in calli compared with calli transformed with empty pRI101 vector (Fig. 2g). We then treated the calli with 1 mM GSNO and evaluated *MdACS1* and *MdACO1* expression, as well as ethylene production. The latter was significantly higher in *MdERF5*-silenced calli compared with the control calli (Fig. 2h) and *MdACS1* expression

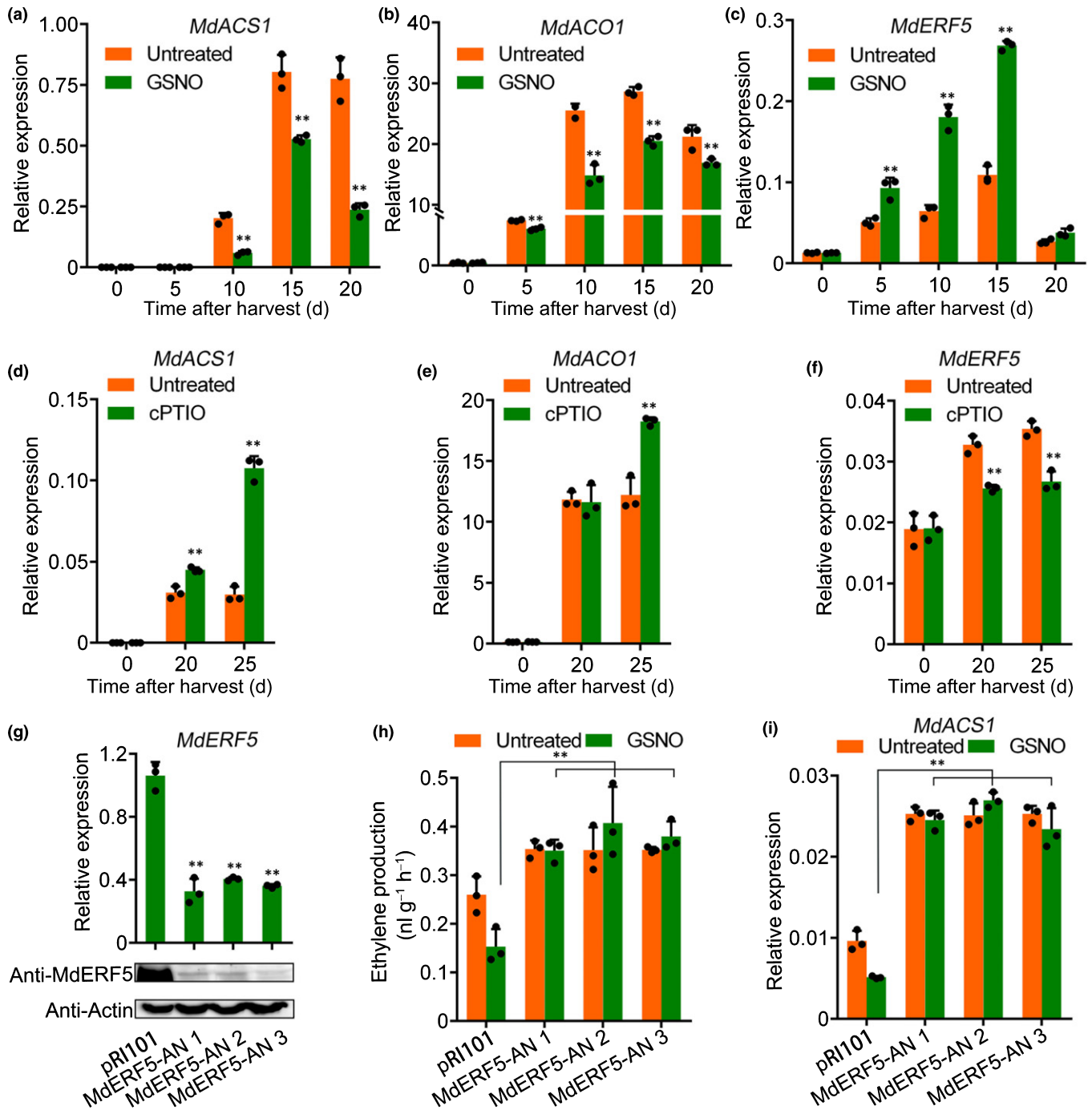


Fig. 2 Nitric oxide (NO) activates the expression of *MdERF5* (ERF, Ethylene Response Factor). (a–c) Quantitative real-time (qRT)-PCR was used to examine *MdACS1* (a), *MdACO1* (b) and *MdERF5* (c) expression in *S*-nitrosoglutathione (GSNO)-treated fruit (1-aminocyclopropane-1-carboxylic acid (ACC) synthase (ACS) and oxidase (ACO)). (d–f) qRT-PCR was used to examine *MdACS1* (d), *MdACO1* (e) and *MdERF5* (f) expression in NO-scavenger 2-(4-carboxyphenyl)-4,4,5,5-tetramethyl-imidazole-1-oxyl-3-oxide (cPTIO)-treated fruit. Untreated, fruit not receiving any treatment; GSNO, fruit treated with GSNO; cPTIO, fruit treated with cPTIO. Numbers under the x-axes of (a–f) indicate the duration of storage (d) at room temperature after harvest; 0 under the x-axes of (d–f) indicates the day of commercial harvest; 0 under the x-axes of (d–f) indicates the day of harvesting at 130 d after full bloom. For qRT-PCR analysis, three biological replicates were analyzed as described in the Materials and Methods section. Values represent means \pm SE. Each dot represents a biologically independent sample. Statistical significance was determined using a Student's *t*-test (**, $P < 0.01$). (g–i) *MdERF5* expression was silenced using RNAi technology in apple fruit calli (*MdERF5*-AN) via *Agrobacterium tumefaciens*-mediated transformation. *MdERF5* expression was investigated by qRT-PCR and immunoblot analysis (g). Anti-plant Actin mouse monoclonal antibody (anti-Actin) was used as a loading control. *MdERF5*-suppressed calli were treated with GSNO as described in the Materials and Methods section, and ethylene production was measured. Values represent means \pm SE. Each dot represents a biologically independent sample. Statistical significance was determined using a Student's *t*-test (**, $P < 0.01$). (h). *MdACS1* expression was investigated by qRT-PCR in *MdERF5*-suppressed calli (i). Calli infected with empty vector (pRI101) were used as controls.

was suppressed, consistent with ethylene production (Fig. 2i), whereas *MdACO1* expression showed no significant difference between *MdERF5*-silenced and control calli (Fig. S4). These results indicated that *MdERF5* is essential for NO-suppressed ethylene biosynthesis in apple fruit, and that it may regulate *MdACS1*, but not *MdACO1* transcription.

MdERF5 is a nucleocytoplasmic protein

In order to further analyze the function of MdERF5, we investigated its subcellular localization. To avoid any mis-localization caused by the strong Super promoter that was used, we co-expressed MdERF5 fused to GFP under its native promoter (*ProMdERF5::MdERF5-GFP*), together with an mCherry-labeled nuclear marker (NF-YA4-mCherry) (Zhang *et al.*, 2019) in wild tobacco (*N. benthamiana*) leaves. MdERF5 exclusively localized to the nucleus in mock-infiltrated leaves (Figs 3a, S5). However, when tobacco leaves were subjected to GSNO or SNP treatment for 2 h, most of the green fluorescence was observed in the cytoplasm based on the overlapping red fluorescence with an mCherry-labeled plasma membrane marker protein (PM-mCherry) (Fig. 3b). The strength of the GFP fluorescent signals in the cytoplasm increased with time (Figs 3a, S5).

In order to determine whether the distribution of MdERF5 also was affected by NO in fruit, we first generated a polyclonal anti-MdERF5 antibody, which we used in an immunoblot analysis of total fruit proteins and found that MdERF5 levels increased during storage and GSNO treatment elevated MdERF5 levels (Fig. 3c). Next, we performed another immunoblot analysis with nuclear and cytoplasmic protein extracts from fruit. The MdERF5 levels increased gradually during storage and GSNO treatment also increased the abundance of MdERF5 in the nucleus (Fig. 3d). The same is true of the MdERF5 levels in the cytoplasm (Fig. 3e). These results suggested that MdERF5 levels increase in both the nucleus and cytoplasm in response to GSNO treatment in fruit.

The subcellular distribution of MdERF5 is related to the presence of the protein phosphatase MdPP2C57

Previous studies have shown that the subcellular distribution of nucleocytoplasmic proteins is related to their phosphorylation status (Ryu *et al.*, 2007; Zhang *et al.*, 2019). We therefore tested the hypothesis that NO causes changes in MdERF5 phosphorylation and affects its subcellular distribution. This was done *in planta* using a phos-tag reagent to label total protein extracts from fruit. We observed that the MdERF5 phosphorylation level increased gradually during fruit storage and that GSNO treatment suppressed MdERF5 phosphorylation (Fig. 3f; the original figure is Fig. S6), suggesting that NO lowered the phosphorylation level of MdERF5.

In order to test whether the dephosphorylation and subsequent plasma membrane localization of MdERF5 was mediated by a protein phosphatase (PP), we monitored the NO-induced plasma membrane localization of MdERF5 in the presence of okadaic acid (OA) or sanguinarine chloride (SC), which inhibit Type-1 and Type-2A serine/threonine protein

phosphatases (PP1 and PP2A) and Type-2C serine/threonine protein phosphatases (PP2C), respectively. MdERF5 was observed to localize to the nucleus and plasma membrane when treated with GSNO alone (Fig. 4a); however, it was localized to the nucleus and not the plasma membrane when treated with SC followed by GSNO (SC+GSNO) (Fig. 4a). This suggested that the SC treatment inhibited the translocation of MdERF5 from the nucleus to the plasma membrane even in the presence of GSNO, whereas treatment with OA had no effect on the translocation (Fig. S7). These results suggested that PP2C-type phosphatases mediate the NO-induced plasma membrane translocation of MdERF5.

In order to further explore the molecular basis by which NO attenuates MdERF5 phosphorylation, we analyzed the above-mentioned RNA-seq data (Table S2) and identified an annotated 2C-type protein phosphatase gene, *MdPP2C57*, whose expression was activated by GSNO treatment in apple fruit (Fig. 4b; Table S4) and gradually decreased during fruit development (Fig. 4c). We then analyzed the subcellular localization of MdPP2C57 by expressing the *MdPP2C57* coding sequence (CDS) fused to a GFP tag under control of its native promoter (*ProMdPP2C57::MdPP2C57-GFP*) in *N. benthamiana* leaves. We observed that MdPP2C57 localized to the nucleus, and that its subcellular distribution was not affected by GSNO treatment (Fig. 4d).

Next, we investigated whether MdPP2C57 and MdERF5 physically interact using a Yeast two-hybrid (Y2H) assay, and found that the two proteins did indeed interact in yeast cells (Fig. 5a). We then divided the predicted MdERF5 coding region into three fragments (MdERF5N, MdERF5D and MdERF5C), and observed that MdPP2C57 interacted with MdERF5N and MdERF5D in Y2H yeast (Fig. S8). We also checked their co-localization, and found them to be co-localized only in the nucleus (Fig. S9). A BiFC assay was performed to determine where MdPP2C57 and MdERF5 interact *in planta*. Constructs containing MdPP2C57 cloned into the pSPYNE-35S vector (*MdPP2C57-nYFP*) and MdERF5 cloned into the pSPYCE-35S vector (*MdERF5-cYFP*) were co-infiltrated into *N. benthamiana* leaves, and the infiltrated leaves were treated with GSNO. The observed fluorescence pattern showed that MdPP2C57 interacted with MdERF5 in the nucleus (Fig. 5b), and that GSNO treatment did not change the localization of the MdPP2C57–MdERF5 interaction (Fig. 5b). To confirm this result *in vivo*, we conducted a firefly luciferase (Luc) complementation imaging assay. Constructs containing MdPP2C57 fused with the N-terminus of Luc (*MdPP2C57-nLuc*), and the C-terminus of Luc fused with MdERF5 (*cLuc-MdERF5*) were co-infiltrated into *N. benthamiana* leaves and the infiltrated leaves were treated with GSNO. A strong luminescence signal was detected in the *MdPP2C57-nLuc/cLuc-MdERF5* co-expressing regions (Fig. 5c, region 1) but not in the negative controls (Fig. 5c, regions 3–8), and a stronger luminescence signal was observed in the *MdPP2C57-nLuc/cLuc-MdERF5* co-expressing regions following GSNO treatment (Fig. 5c, region 2). These results verified that MdPP2C57 interacts with MdERF5 *in vivo* and that NO activates their interaction.

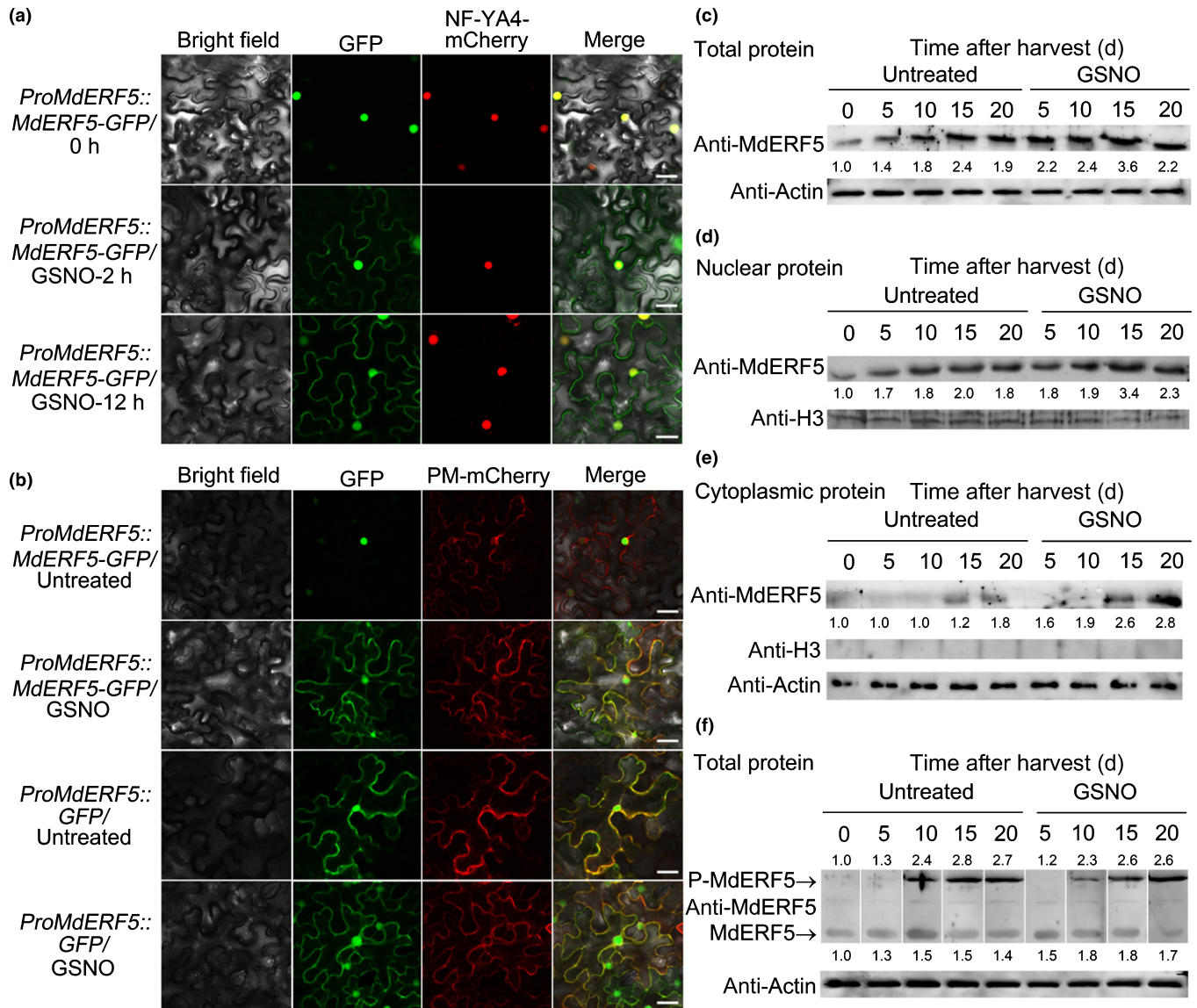


Fig. 3 Nitric oxide (NO) mediates the nucleocytoplasmic shuttling of MdERF5 (ERF, ETHYLENE RESPONSE FACTOR). (a, b) Confocal and brightfield images of *Nicotiana benthamiana* cells expressing *MdERF5* treated with *S*-nitrosoglutathione (GSNO). *MdERF5* was driven by its native promoter and green fluorescent protein (GFP) was fused to its C terminus (*ProMdERF5::MdERF5-GFP*). An mCherry-labeled nuclear marker (*NF-YA4-mCherry*) was expressed together with *ProMdERF5::MdERF5-GFP*. The time since GSNO-treatment is indicated (0, 2 and 12 h) (a). An mCherry-labeled plasma membrane marker (*PM-mCherry*, CD3-1007) was expressed together with *ProMdERF5::MdERF5-GFP* (b). Co-infiltration of *ProMdERF5::GFP* with *PM-mCherry* represents the control. Untreated, tobacco leaves not receiving any treatment; GSNO, tobacco leaves treated with GSNO. The experiment was performed three times independently, and representative results are shown. Bar, 50 μ M. (c–e) MdERF5 protein levels were analyzed by immunoblot analysis: (c) total MdERF5; (d) nuclear MdERF5; (e) cytoplasmic MdERF5. Anti-H3 was used as a nuclear protein control; anti-Actin was used as a cytoplasmic protein control. (f) Phosphorylated MdERF5 protein levels were analyzed by phos-tag gel analysis. P-MdERF5 bands indicate phosphorylated MdERF5 protein; MdERF5 bands indicate unphosphorylated MdERF5 protein. Anti-Actin was used as a loading control. Untreated, fruit not receiving any treatment; GSNO, fruit treated with GSNO. Numbers under the line indicate the duration of storage (d) at room temperature after harvest; 0 indicates the day of commercial harvest.

We then performed an *in vitro* dephosphorylation assay to detect if MdPP2C57 dephosphorylates MdERF5. Recombinant GST-tagged MdPP2C57 (MdPP2C57-GST) was purified and incubated with MdERF5-3xFlag immunoprecipitated from *N. benthamiana* in a phosphatase reaction buffer. GST protein was used as the negative control. A strong MdERF5 phosphorylation band was detected in the presence of GST protein, whereas

an unphosphorylated as well as a phosphorylated MdERF5 band was detected in the presence of MdPP2C57-GST (Fig. 5d). To obtain further evidence that MdPP2C57 dephosphorylates MdERF5, we characterized MdERF5 phosphorylation using a phos-tag reagent with anti-Flag immunoprecipitated proteins from total protein extracts. The *MdERF5* CDS was ligated downstream of a 3xFlag tag under control of the *35S* promoter

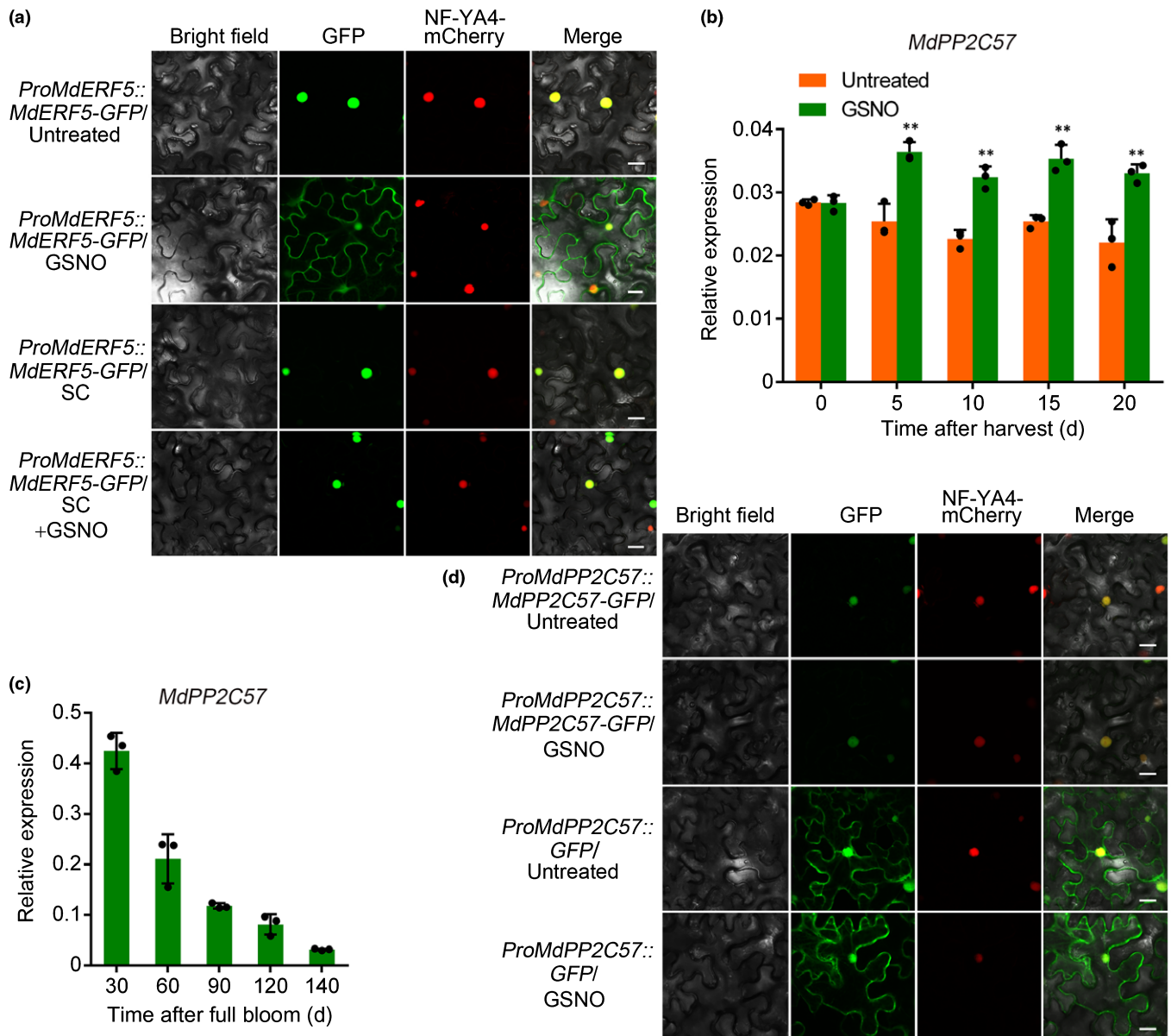


Fig. 4 Nitric oxide (NO)-activated protein phosphatase *MdPP2C57* transcription. (a) Confocal and brightfield images of *Nicotiana benthamiana* cells expressing *MdERF5* treated with the Type-2C serine/threonine protein phosphatase (PP2C)-specific inhibitor, sanguinarine chloride (SC) and S-nitrosoglutathione (GSNO) (ERF, EHTYLENE RESPONSE FACTOR). *MdERF5* was driven by its native promoter and green fluorescent protein (GFP) was fused to its C-terminus (*ProMdERF5::MdERF5-GFP*). An mCherry-labeled nuclear marker (*NF-YA4-mCherry*) was expressed together with *ProMdERF5::MdERF5-GFP*. Bar, 50 μ M. (b, c) *MdPP2C57* expression by qRT-PCR in GSNO-treated fruit (b) and during apple fruit development in 2019 (c). Untreated, fruit not receiving any treatment; GSNO, fruit treated with GSNO. For qRT-PCR analysis, three biological replicates were analyzed as described in the Materials and Methods section. Values represent means \pm SE. Each dot represents a biologically independent sample. Statistical significance was determined using a Student's *t*-test (**, $P < 0.01$). (d) Confocal and brightfield images of *N. benthamiana* cells expressing *MdPP2C57* treated with GSNO. *MdPP2C57* was driven by its native promoter and GFP was fused to its C-terminus (*ProMdPP2C57::MdPP2C57-GFP*). *NF-YA4-mCherry* was expressed together with *ProMdPP2C57::MdPP2C57-GFP*. Co-infiltration of *ProMdPP2C57::GFP* and *NF-YA4-mCherry* represents the control. Untreated, tobacco leaves not receiving any treatment; GSNO, tobacco leaves treated with GSNO alone; SC, tobacco leaves treated with SC alone; SC+GSNO, tobacco leaves treated with SC followed by GSNO. The experiment was performed three times independently, and representative results are shown. Bar, 50 μ M.

(*MdERF5-3xFlag*) and overexpressed with another construct containing the *MdPP2C57* CDS ligated into the pRI101 vector without any tag (*MdPP2C57-pRI101*) in *N. benthamiana* leaves. A strong *MdERF5* phosphorylation band was detected in mock-infiltrated leaves, whereas an un-phosphorylated as well as a

phosphorylated *MdERF5* band was detected in the presence of *MdPP2C57-pRI101* (Fig. 5e). These results suggested that *MdPP2C57* dephosphorylates *MdERF5*.

Given the above data, we hypothesized that the subcellular distribution of *MdERF5* is related to *MdPP2C57*. To investigate

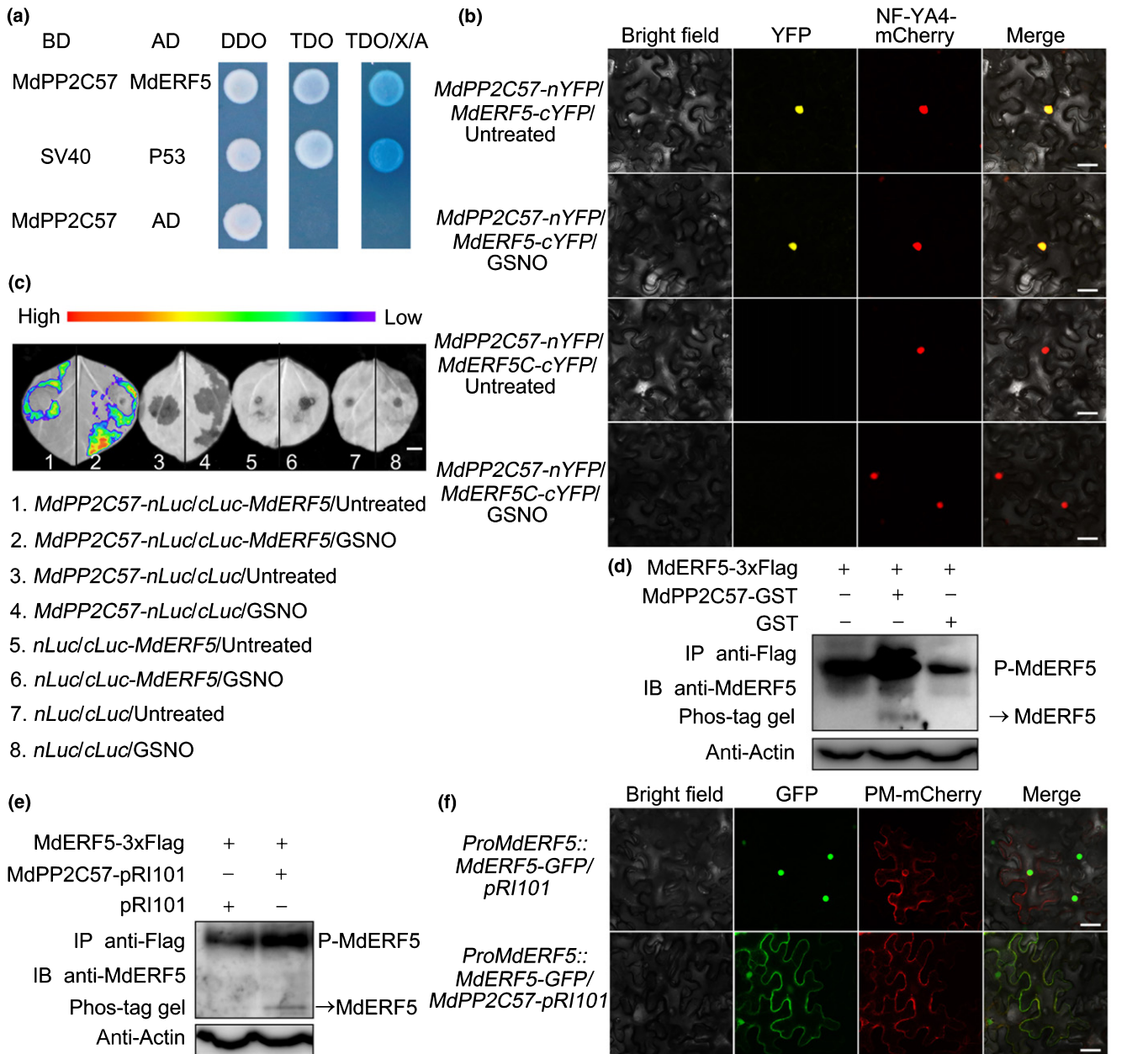


Fig. 5 Protein phosphatase MdPP2C57 mediates the nucleocytoplasmic shuttling of MdERF5 (EF, ETHYLENE RESPONSE FACTOR). (a) The interaction between MdPP2C57 and MdERF5 was investigated using a yeast two-hybrid assay. DDO, SD medium lacking Trp and Leu; TDO, SD medium lacking Trp, Leu and His; TDO/X/A, TDO medium containing X- α -gal and aureobasidin A. SV40 and P53 were used as positive controls, MdPP2C57-BD and AD vectors as negative controls. Blue indicates protein interaction. (b) MdPP2C57–MdERF5 interaction in a bimolecular fluorescence complementation (BiFC) assay. Tobacco leaves were co-infiltrated with *MdERF5-cYFP* and *MdPP2C57-nYFP* constructs and kept in the dark for 48 h, and then 100 μ M S-nitrosoglutathione (GSNO) was injected into the infiltrated leaves as described in the Materials and Methods section (YFP, yellow fluorescent protein). *NF-YA4-mCherry* was used as a nuclear marker. *MdERF5C-cYFP* co-transformed with *MdPP2C57-nYFP* was used as negative control. Bar, 50 μ m. (c) A firefly luciferase complementation imaging assay showing that GSNO treatment enhanced MdERF5–MdACO1 interaction in tobacco leaves. *Agrobacterium tumefaciens* strain EHA105 harboring different constructs was infiltrated into tobacco leaves. Untreated, tobacco leaves not receiving any treatment; GSNO, tobacco leaves treated with GSNO. Luciferase activities were recorded in these regions 3 d after infiltration. Bar, 1 cm. (d, e) A phos-tag gel was used to analyze MdERF5 protein phosphorylation. The *MdPP2C57* coding sequence (CDS) was inserted into the pGEX4T-1 vector downstream from glutathione S-transferase (GST). Recombinant fusion proteins were purified. MdERF5-3xFlag protein immunoprecipitated (IP) from *Nicotiana benthamiana* was incubated with MdPP2C57-GST in phosphatase reaction buffer. Co-incubation of MdERF5-3xFlag with GST represents the control (d). The *MdERF5* CDS was ligated downstream of 3xFlag peptide tags under the control of the 35S promoter in the pRI101 vector (*MdERF5-3xFlag*) and expressed with *MdPP2C57-pRI101* in *N. benthamiana*. Co-expression of *MdERF5-3xFlag* with *pRI101* represents the control (e). Anti-Actin was used as a loading control. P-MdERF5 bands indicate phosphorylated MdERF5 protein. MdERF5 bands indicate unphosphorylated MdERF5 protein. (f) MdPP2C57 induced the movement of MdERF5 from the nucleus to the plasma membrane. *MdERF5* was driven by its native promoter and green fluorescent protein (GFP) was fused to its C-terminus (*ProMdERF5::MdERF5-GFP*). An overexpression *MdPP2C57* vector (*MdPP2C57-pRI101*) was expressed together with *ProMdERF5::MdERF5-GFP*. Empty vector *pRI101* was used as a control. *PM-mCherry* was used as a plasma membrane marker. Bar, 50 μ m.

this, we co-infiltrated the *ProMdERF5::MdERF5-GFP* construct and *MdPP2C57-pRI101* into *N. benthamiana* leaves. We observed that the presence of the MdPP2C57 induced the movement of MdERF5 from the nucleus to the plasma membrane (Figs 5f, S10). These results suggested that MdPP2C57 affects the MdERF5 phosphorylation level, thereby mediating nucleocytoplasmic shuttling of MdERF5.

MdERF5 Ser260 is critical for MdPP2C57-induced nucleocytoplasmic shuttling of MdERF5

Nuclear localization signal (NLS) is important for the distribution of transcription factor in the cell. The nuclear export of MdERF5 mediated by NO might be related to its NLS. Amino acid residues 259–269 were predicted to be a putative NLS of MdERF5 (Fig. S11). We then deleted the NSL of MdERF5, resulting in construct *ProMdERF5::MdERF5-ΔNLS-GFP* under its native promoter and analyzed its subcellular localization in *N. benthamiana* leaves. The results showed that deletion of the NLS domain caused broad distribution of MdERF5-ΔNLS-GFP throughout the cell (Fig. 6a, second panel).

We have demonstrated that the nucleocytoplasmic distribution of MdERF5 is related to its phosphorylation status (Fig. 5). Then we paid attention to the putative phosphorylation site at the NSL domain and observed only Ser260 residue (Fig. S11). To determine whether phosphorylation at Ser260 influences MdERF5 subcellular localization, we created phosphorylation-deficient and phosphomimetic forms of MdERF5 by introducing mutations of Ser260 to either Ala (S260A) or Asp (S260D), and investigated their subcellular distribution in *N. benthamiana* leaves and maize (*Zea mays*) leaves protoplasts. Green fluorescence of *ProMdERF5::MdERF5^{S260A}-GFP* was observed to be broadly distributed throughout the cell (Fig. 6a,b, third panel); whereas green fluorescence of *ProMdERF5::MdERF5^{S260D}-GFP* mainly localized in the nucleus (Fig. 6a,b, bottom panel). These results indicate that dephosphorylation of MdERF5 at Ser260 is sufficient to promote its nucleocytoplasmic shuttling.

In order to test whether MdPP2C57 acts on MdERF5 Ser260 to regulate the nuclear export of MdERF5, we co-infiltrated the constructs *ProMdERF5::MdERF5^{S260D}-GFP* and *MdPP2C57-pRI101* into *N. benthamiana* leaves. We observed that the presence of MdPP2C57 no longer induced the movement of MdERF5 from the nucleus to the cytoplasm (Fig. 6c). Taken together, we conclude that MdPP2C57 induces the dephosphorylation of MdERF5 at Ser260 to result in the nucleocytoplasmic shuttling of MdERF5.

MdERF5 interacts with MdACO1 and suppresses its activity

In order to further characterize the putative role of MdERF5 in NO-suppressed ethylene biosynthesis, we screened an apple fruit cDNA library in a Y2H screening system using MdERF5 as the bait. A total of 86 positive clones were identified, corresponding to 19 genes; one of which encoded MdACO1, a key ethylene biosynthesis enzyme. The potential MdERF5 and MdACO1 interaction was confirmed using a Y2H assay (Fig. 7a) and further

validated using a pull-down assay involving MdERF5-His and MdACO1-GST peptide tagged fusion proteins (Fig. 7b). A co-IP assay was employed to confirm this result, in which apple fruit calli were transformed with a construct harboring a sequence encoding a GFP tag fused to the *MdACO1* CDS (MdACO1-GFP). MdERF5 was detected in extracts of MdACO1-GFP transgenic calli, confirming the *in vivo* interaction between MdACO1 and MdERF5 (Fig. 7c).

Next, we investigated the subcellular localization of MdACO1. Constructs containing the *MdACO1* CDS fused to a GFP peptide tag and expressed under the control of its native promoter (*ProMdACO1::MdACO1-GFP*) were infiltrated into *N. benthamiana* leaves and fluorescence imaging of the leaves suggested that MdACO1 is a nucleocytoplasmic protein, and that its subcellular distribution is not affected by NO (Fig. S12a,b). We also found that MdERF5 co-localized with MdACO1 only in the nucleus under normal conditions, whereas after GSNO treatment, MdERF5 and MdACO1 localized to both the cytoplasm and nucleus (Fig. S13). In a BiFC assay, MdERF5 interacted with MdACO1 only in the nucleus, and following GSNO treatment, the fluorescent signal corresponding to a MdERF5–MdACO1 interaction was observed in both the cytoplasm and nucleus (Fig. 7d).

We also performed a Luc complementation imaging assay to investigate how NO affects the MdERF5–MdACO1 interaction. Constructs containing MdACO1 fused with the N-terminus of Luc (*MdACO1-nLuc*) and the C-terminus of Luc fused with MdERF5 (*cLuc-MdERF5*) were co-infiltrated into *N. benthamiana* leaves. A luminescence signal was detected in the *MdACO1-nLuc/cLuc-MdERF5* co-expressing region (Fig. 7e, Region 1) but not in the negative controls (Fig. 7e, Regions 3, 5 and 7). Following GSNO treatment, a stronger luminescence signal was detected (Fig. 7e, Region 2) but not in the negative controls (Fig. 7e, Regions 4, 6 and 8). The results of a co-IP assay were consistent with this result in *N. benthamiana* leaves, in which MdERF5-Myc and MdACO1-GFP were overexpressed and treated with GSNO. MdERF5-Myc was detected in the MdACO1-GFP immunoprecipitated extract, and GSNO treatment enhanced the signal (Fig. S14), suggesting a MdERF5–MdACO1 protein interaction. Taken together these results indicated that NO promotes the MdERF5–MdACO1 interaction.

We then divided the predicted MdACO1 CDS into four fragments (MdACO1N, MdACO1M, MdACO1D and MdACO1C), and performed a Y2H assay with MdERF5N, MdERF5D and MdERF5C. We observed that MdERF5N interacted with MdACO1N, MdACO1D and MdACO1C (Fig. 7f). We noted that the MdACO1D fragment contains a putative Fe (II) binding site (Fig. S15) that is essential for ACO enzyme activity (Ji *et al.*, 2021). To investigate whether the MdERF5–MdACO1 interaction affects the enzymatic activity of MdACO1 in the cytoplasm where ACO converts ACC to ethylene, we first purified recombinant poly-histidine-tagged MdACO1 (MdACO1-His) and recombinant GST-tagged MdERF5 (MdERF5-GST). We next mixed purified MdACO1 with different amounts of purified MdERF5 in a reaction buffer and measured ethylene production. Purified MdACO1 with different amounts of purified GST protein was used as a control. We

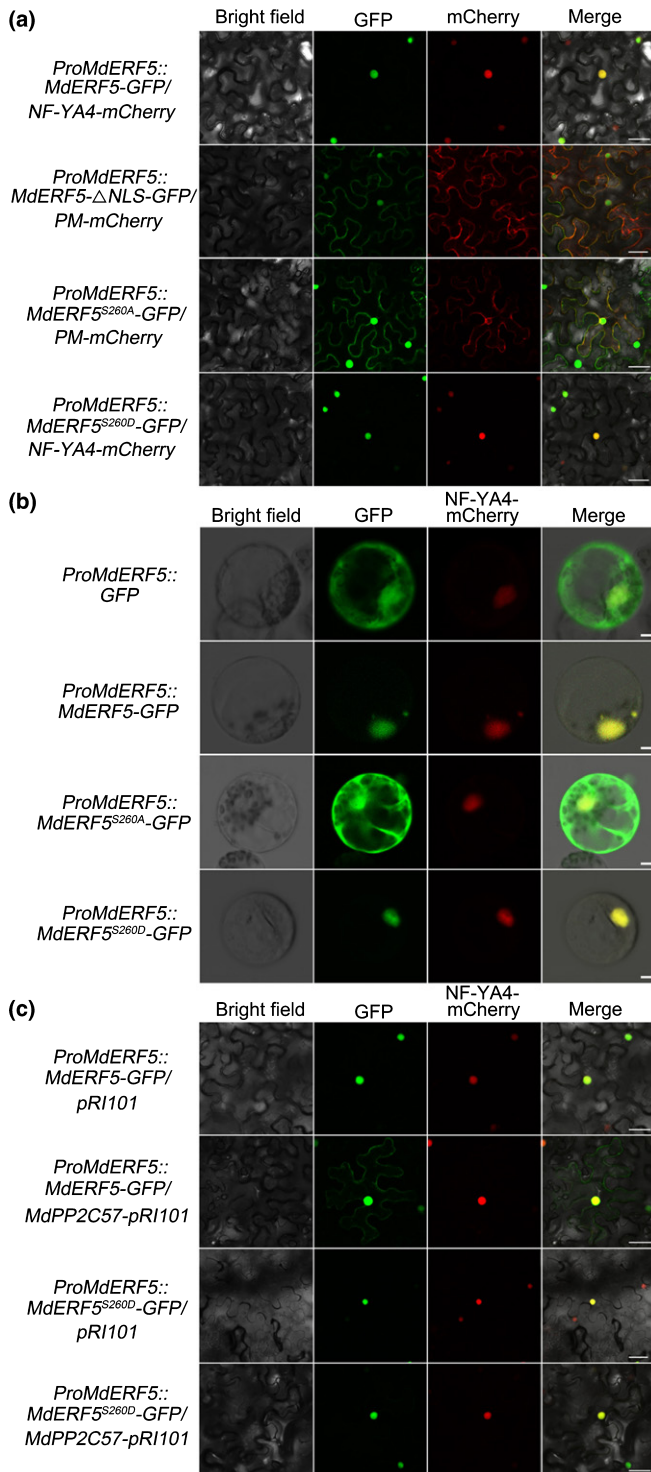


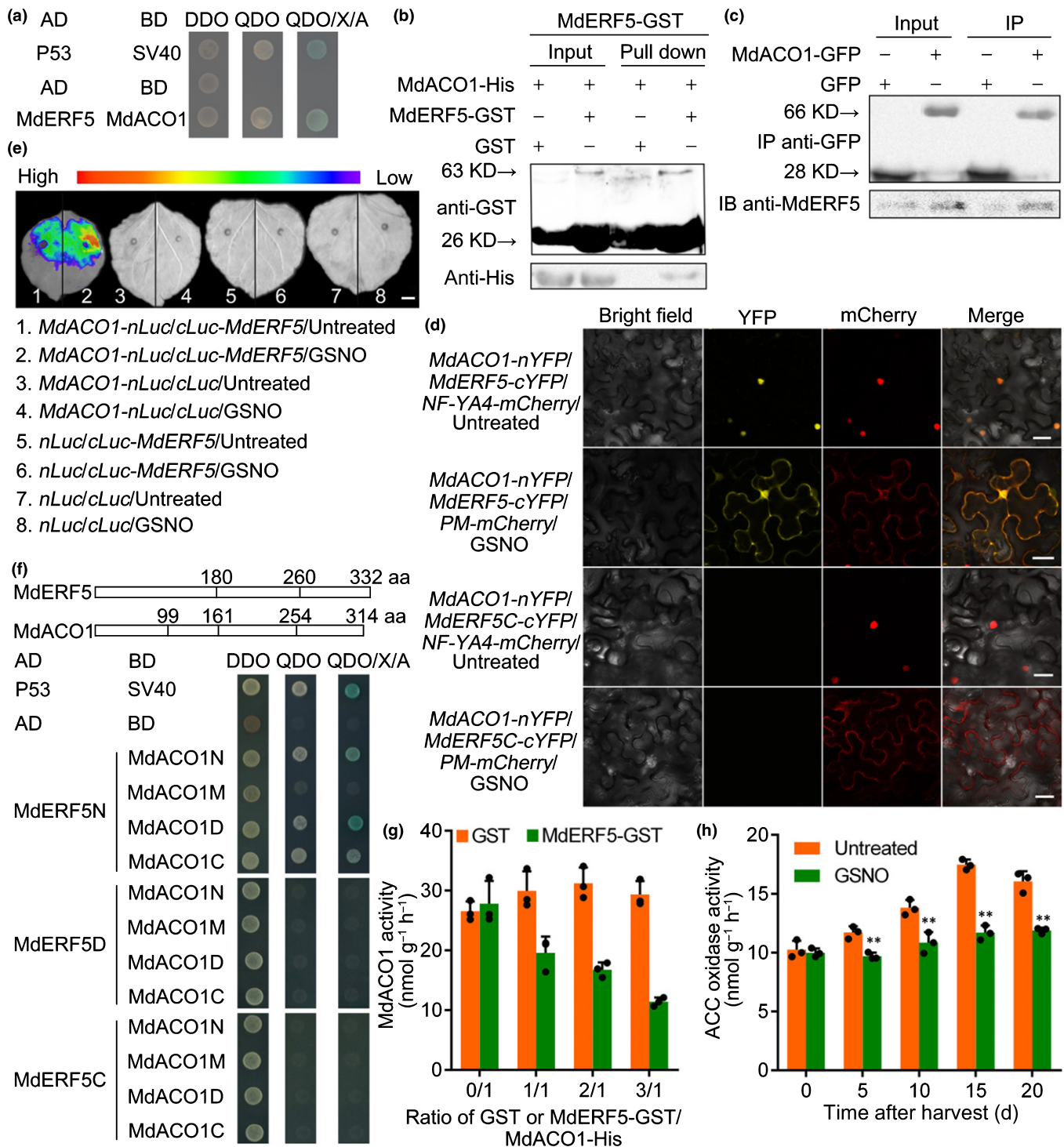
Fig. 6 Protein phosphatase MdPP2C57 mediates the nucleocytoplasmic shuttling of MdERF5 via dephosphorylating Ser260 (ERF, ETHYLENE RESPONSE FACTOR). (a) Subcellular localization of MdERF5 in *Nicotiana benthamiana* leaves. Green fluorescent protein (GFP) was fused to the C-terminus of MdERF5, MdERF5-ΔNLS, MdERF5^{S260A} and MdERF5^{S260D} under the promoter of MdERF5. An mCherry-labeled nuclear marker (NF-YA4-mCherry) was co-infiltrated with ProMdERF5::MdERF5-GFP and ProMdERF5::MdERF5^{S260D}-GFP, and an mCherry-labeled plasma membrane marker (PM-mCherry, CD3-1007) was expressed together with ProMdERF5::MdERF5-ΔNLS-GFP and ProMdERF5::MdERF5^{S260A}-GFP. ΔNLS, deletion of the nuclear localization signal (NLS) domain; S260A, Ser260 to Ala (phosphodeficient form); S260D, Ser260 to Asp (phosphomimetic form). Bar, 50 μM. (b) Subcellular localization of MdERF5 in protoplasts of maize leaves. NF-YA4-mCherry was co-infiltrated with ProMdERF5-GFP, ProMdERF5::MdERF5-GFP, ProMdERF5::MdERF5^{S260A}-GFP and ProMdERF5::MdERF5^{S260D}-GFP. ProMdERF5-GFP was used as a control. Bar, 5 μM. (c) MdPP2C57 does not mediate the nucleocytoplasmic shuttling of MdERF5^{S260D}. MdPP2C57-pRI101 was co-expressed together with ProMdERF5::MdERF5^{S260D}-GFP. Empty vector pRI101 was used as a control together with ProMdERF5::MdERF5^{S260D}-GFP. NF-YA4-mCherry was used as a nuclear marker. Bar, 50 μM. These experiments were performed independently three times, and representative results are shown.

NO suppresses MdACO1 enzyme activity via enhancement of the MdERF5–MdACO1 interaction in the cytoplasm.

NO-activated MdERF5 suppresses the expression of *MdACS1*

We performed a Y1H assay and confirmed that MdERF5 bound to the *MdACS1* promoter (Fig. 8a). To further confirm this, we purified the full-length MdERF5 protein and performed an electrophoretic mobility shift assay (EMSA) with fragments of biotin-labeled *MdACS1* promoter containing the DRE (dehydration-related element) motif as the labeled probe. MdERF5 bound to the *MdACS1* promoter (Fig. 8b, lane 2), and when an unlabeled probe containing five mutated nucleotides was used as a competitor, the binding of MdERF5 to the *MdACS1* promoter was unaffected (Fig. 8b, lanes 5 and 6). When the *MdACS1* promoter was divided into various fragments, MdERF5 bound to the fragment containing the DRE motif (Fig. S17a). Likewise, when the MdERF5N, MdERF5D and MdERF5C fragments were used in a Y1H assay, we found that the MdERF5D fragment bound to the *MdACS1* promoter (Fig. S17b). These results indicated that the MdERF5 ERF domain binds to the *MdACS1* promoter DRE motif *in vitro*. *In vivo* verification was performed with a ChIP-PCR assay. The *MdERF5* CDS fused to a sequence encoding a GFP peptide tag was overexpressed in apple fruit calli (Fig. S18). The presence of MdERF5 substantially enhanced the PCR-based detection of the *MdACS1* promoter (Fig. 8c), indicating that MdERF5 also binds to the *MdACS1* promoter *in vivo*. Furthermore, when the regulation of the *MdACS1* promoter by MdERF5 was examined in *N. benthamiana* leaves co-transformed with *Pro35S::MdERF5* and *ProMdACS1::GUS* constructs it was found, using a β-glucuronidase (GUS) transactivation assay, that MdERF5 suppresses *MdACS1* promoter activity (Fig. 8d). When GSNO was applied to the *N. benthamiana* leaves, the GUS signal was further

observed that MdACO1 activity gradually declined with increasing amounts of MdERF5 (Fig. 7g), suggesting suppression of MdACO1 activity through direct interaction with MdERF5. To test whether MdERF5 affects MdACO1 activity *in vivo*, we also measured ACO enzymatic activity in extracts from apple fruit, in studies in 2017 (Fig. S16a), 2018 (Fig. S16b) and 2019 (Fig. 7h). We found that GSNO treatment significantly inhibited ACO enzyme activity. Taken together these findings suggested that



reduced (Fig. 8d). Taken together, these results suggested that MdERF5 directly suppressed *MdACS1* transcription and that NO strengthens this suppression.

Given the interaction between MdERF5 and MdPP2C57 or MdACO1 in the nucleus (Figs 5b, 7d), we investigated the effect of this interaction on MdERF5 binding to the *MdACS1* promoter. EMSA analysis suggested that the increase in MdACO1 abundance did not affect the MdERF5 binding to the *MdACS1*

promoter (Fig. S19). However, we did observe that the increase in MdPP2C57 abundance promoted MdERF5 binding to the *MdACS1* promoter in an EMSA assay (Fig. 8e). Likewise, in a GUS transactivation assay, the GUS signal was further reduced when *Pro35S::MdERF5* and *Pro35S::MdPP2C57* were co-transformed with *ProMdACS1::GUS* (Fig. 8f). These results suggested that the MdERF5–MdPP2C57 interaction promotes MdERF5 binding to the *MdACS1* promoter. In addition, we also

Fig. 7 Nitric oxide (NO)-activated ETHYLENE RESPONSE FACTOR (MdERF5) interacts with 1-aminocyclopropane-1-carboxylic acid (ACC) oxidase 1 (MdACO1) and inhibits MdACO1 enzyme activity. (a) The interaction between MdERF5 and MdACO1 was investigated using a yeast two-hybrid (Y2H) assay. DDO, SD medium lacking Trp and Leu; QDO, SD medium lacking Trp, Leu, His and Ade; QDO/X/A, QDO medium containing X- α -gal and aureobasidin A. SV40 and P53 were used as positive controls, and AD vectors as negative controls. Blue indicates protein interaction. (b) Recombinant His-tagged MdACO1 and glutathione S-transferase (GST)-tagged MdERF5 were purified and used in a pull-down analysis. His and GST antibodies were used for immunoblot analysis. The band detected by the His antibody in the pull-down experiment indicates an interaction between MdACO1 and MdERF5. (c) MdERF5–MdACO1 interaction in a coimmunoprecipitation (co-IP) assay. MdACO1 fused to a GFP tag (MdACO1-GFP) was overexpressed in apple fruit calli and a GFP antibody was used for immunoprecipitation analysis. A MdERF5-specific antibody (anti-MdERF5) was used in an immunoblot analysis. The band detected by anti-MdERF5 in the precipitated protein sample indicates the MdERF5–MdACO1 interaction (right-hand lane). (d) MdERF5–MdACO1 interaction in a bimolecular fluorescence complementation (BiFC) assay. Tobacco leaves were co-infiltrated with *MdERF5-cYFP* and *MdACO1-nYFP* constructs and kept in the dark for 48 h, and then 100 μ M S-nitrosoglutathione (GSNO) was injected into the infiltrated leaves as described in the Materials and Methods section. *NF-YA4-mCherry* was used as a nuclear marker. *MdERF5C-cYFP* with *MdACO1-nYFP* was used as a negative control. Bar, 50 μ M. (e) A firefly luciferase complementation imaging assay showing that GSNO treatment enhanced MdERF5–MdACO1 interaction in tobacco leaves. *Agrobacterium tumefaciens* strain EHA105 harboring different constructs was infiltrated into tobacco leaves. Untreated, tobacco leaves not receiving any treatment; GSNO, tobacco leaves treated with GSNO. Luciferase activities were recorded in these regions 3 d after infiltration. Bar, 1 cm. (f) The MdERF5 and MdACO1 protein sequences were divided into three and four fragments, respectively, and their interaction was investigated using a Y2H assay. (g) The consequence of the MdERF5–MdACO1 interaction on MdACO1 activity was examined by adding increased amounts of the MdERF5 protein. Recombinant GST-tagged MdERF5 and His-tagged MdACO1 were used. GST protein was used as a control. Error bars represent the SE of three independent measurements. Each dot represents a biologically independent sample. (h) ACC oxidase activity in apple fruit treated with GSNO. Apple fruit were collected at the commercial harvest stage in 2019, treated with GSNO, and stored at room temperature for 20 d. Untreated, fruit not receiving any treatment; GSNO, fruit treated with GSNO. Numbers under the x-axes indicate the duration of storage (d) at room temperature after harvest; 0 indicates the day of commercial harvest. Three biological replicates were analyzed as described in Supporting Information Methods S5 section. Values represent means \pm SE. Each dot represents a biologically independent sample. Statistical significance was determined using a Student's *t*-test (**, $P < 0.01$).

analyzed the regulation of different MdERF5 forms on *MdACS1* promoter activity. By co-infiltrating MdERF5, MdERF5^{S260A} or MdERF5^{S260D} effector vector, respectively, and the reporter vector containing the *MdACS1* promoter into tobacco leaves (Fig. 8g), we observed the phosphorylated form of MdERF5 enhanced and the unphosphorylated form weakened its inhibitory activity.

MdERF5 is required for NO-suppressed ethylene biosynthesis in apple fruit

In order to further confirm the role of *MdERF5* in NO-suppressed ethylene biosynthesis, we transiently silenced *MdERF5* in apple fruit. The full *MdERF5* CDS was ligated into the pRI101 vector in the reverse direction (MdERF5-AN), and the resulting construct was introduced into *A. tumefaciens*, cultures of which were infiltrated into fruit that were still attached to trees. Fruit infiltrated with the empty pRI101 vector were used as controls. The infiltrated fruit were harvested 14 d after infiltration (DAI), treated with GSNO, and stored at room temperature for 15 d (Fig. 9). In the silenced *MdERF5* apple fruit, *MdERF5* transcript levels were significantly reduced, compared with the control fruit (Fig. 9b), and they showed significantly higher ethylene production after GSNO treatment, compared with the control fruit (Fig. 9c). In addition, *MdACS1* expression (Fig. 9d) and ACO enzyme activity (Fig. 9e) were higher in MdERF5-AN fruit than in control fruit. We likewise used a transient expression assay to silence *MdERF5* expression in fruit that were harvested at the commercial harvest stage. MdERF5-AN cultures of *A. tumefaciens* were infiltrated into fruit harvested at 145 DAFB, and the infiltrated fruit were treated with GSNO, then stored at room temperature for 20 d (Fig. S20a). Compared with the control fruit, *MdERF5* expression was significantly reduced in the silenced *MdERF5* apple fruit (Fig. S20b), and when we measured

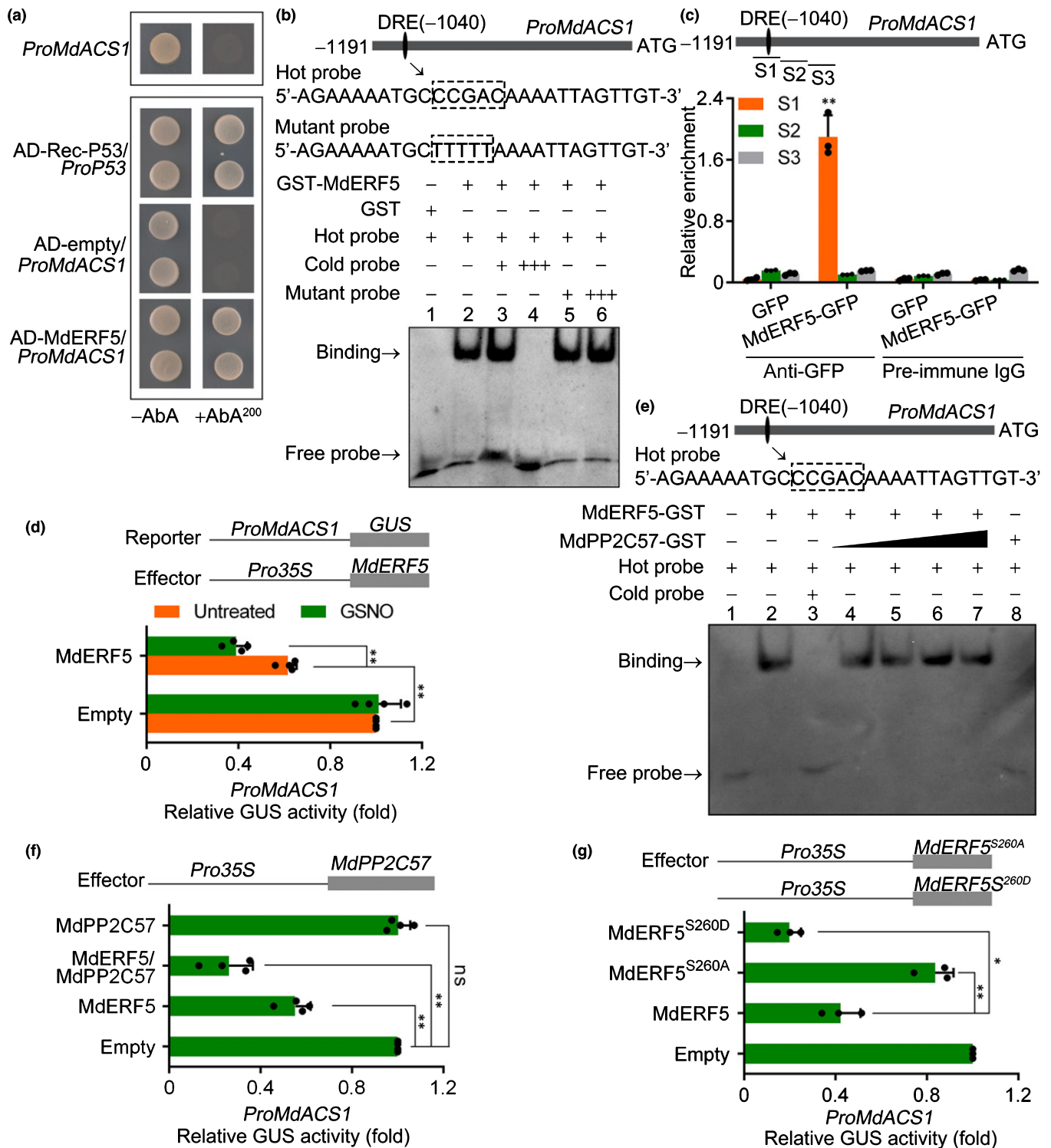
ethylene production, *MdACS1* expression and ACO enzyme activity (Fig. S20c–e), the results were consistent with those from on-the-tree infiltrated fruit. These findings indicated that MdERF5 action is important for NO-suppressed ethylene production in apple fruit.

Discussion

NO suppresses ethylene biosynthesis by transcription factor MdERF5

The effects of nitric oxide (NO) on plant development and stress-related processes by the modulating the action of phytohormones such as cytokinin (Wilhelmova *et al.*, 2006), auxin (Otvos *et al.*, 2005) and ethylene (Ya'acov *et al.*, 1998) have been reported widely. However, although many studies have described the involvement of NO in ethylene biosynthesis in various species, including strawberry (*Fragaria vesca*) (Wills *et al.*, 2000), longan (*Dimocarpus longan*) (Duan *et al.*, 2007), tomato (Zuccarelli *et al.*, 2020) and peach (*Prunus persica*) (Palma *et al.*, 2019), these studies only investigated changes in ethylene production in response to exogenous NO treatment and the expression profile of genes involved in ethylene biosynthesis. The molecular mechanisms by which endogenous NO affects ethylene biosynthesis *in planta* have been unclear.

In this current study, we identified a regulatory mechanism involving the association of the transcription factor (TF) ethylene response factor 5 (MdERF5) with ethylene signaling genes during NO-suppressed ethylene biosynthesis *in planta* in apple (*Malus domestica*). We observed that endogenous NO concentrations gradually decreased during fruit development, during which time ethylene production gradually increased (Li *et al.*, 2015) (Fig. 1a), consistent with NO acting as a ripening suppressor. Through studies of S-nitrosoglutathione (GSNO)-



treated apple fruit, we observed that NO-activated MdERF5 interacted with 1-aminocyclopropane-1-carboxylic acid (ACC) oxidase (MdACO1) in the cytoplasm and suppressed its enzyme activity (Fig. 7) and that MdERF5 bound to the *ACC synthase* (*MdACS1*) promoter in the nucleus, directly suppressing its transcription (Fig. 8).

We observed that MdERF5 suppressed MdACO1 activity by directly interacting with the MdACO1 (Fig. 7a–f). ACO is a member of the Fe(II)-dependent family of oxidases or oxygenases (Zhang *et al.*, 1997) and Fe(II) is a known cofactor catalyzing ethylene biosynthesis (Dong *et al.*, 1992). Previous studies have shown that ACO amino acid sequences are highly conserved

Fig. 8 Nitric oxide (NO)-activated MdERF5 suppresses the transcription of *MdACS1* (ACS, 1-aminocyclopropane-1-carboxylic acid (ACC) synthase; ERF, ETHYLENE RESPONSE FACTOR). (a) Yeast one-hybrid (Y1H) analysis showing that MdERF5 binds to the promoter of *MdACS1* (*ProMdACS1*). AbA (aureobasidin A), a yeast cell growth inhibitor, was used as a screening marker with a basal concentration of 200 ng ml⁻¹. Rec-P53 and the P53-promoter were used as positive controls. The empty vector and the *MdACS1* promoter were used as negative controls. (b) Electrophoretic mobility shift assay (EMSA) showing that MdERF5 binds to the dehydration-related element (DRE) motif in the *MdACS1* promoter. The hot probe was a biotin-labeled fragment of the *MdACS1* promoter containing the DRE motif. The cold probe was a nonlabeled competitive probe (100-, 300-fold that of the hot probe) and the mutant probe was the unlabeled hot probe sequence with CCGAC mutated to TTTT. Glutathione S-transferase (GST)-tagged MdERF5 was purified. (c) Chromatin immunoprecipitation (ChIP)-PCR showing the *in vivo* binding of MdERF5 to the *MdACS1* promoter. Cross-linked chromatin samples were extracted from MdERF5- green fluorescent protein (GFP) overexpressing apple fruit calli (MdERF5-GFP) and precipitated with an anti-GFP antibody. Eluted DNA was used to amplify the sequences neighboring the DRE motif by quantitative (q)-PCR. Three regions (S1, S2 and S3) were investigated. Fruit calli overexpressing GFP were used as negative controls. Values are the percentage of DNA fragments that were co-immunoprecipitated with the GFP antibody or a nonspecific antibody (pre-immune rabbit IgG) relative to the input DNA. The ChIP assay was repeated three times and the enriched DNA fragments in each ChIP were used as one biological replicate for qPCR. Values represent means ± SE. Each dot represents a biologically independent sample. Asterisks indicate significantly different values (**, *P* < 0.01). (d) β-glucuronidase (GUS) activity analysis showing that MdERF5 suppresses the *MdACS1* promoter. The MdERF5 effector vector and the reporter vector containing the *MdACS1* promoter were infiltrated into tobacco leaves to analyze the regulation of GUS activity. Untreated, tobacco leaves not receiving any treatment; GSNO, tobacco leaves treated with S-nitrosoglutathione (GSNO). Three independent transfection experiments were performed. Values represent means ± SE. Each dot represents a biologically independent sample. Asterisks indicate significantly different values (**, *P* < 0.01). (e) Electrophoretic mobility shift assay (EMSA) showing that MdERF5 binds to the dehydration-related element (DRE) motif of the *MdACS1* promoter (lane 2). Increasing amounts of MdPP2C57 enhanced MdERF5 binding to the *MdACS1* promoter (lanes 4–7). GST-tagged MdERF5 and MdPP2C57 were purified. The DRE motif CCGAC is indicated by a dashed box. (f) GUS activity analysis showing that MdERF5–MdPP2C57 interaction promotes MdERF5 binding to the *MdACS1* promoter. Values represent means ± SE. Each dot represents a biologically independent sample. Asterisks indicate significantly different values (**, *P* < 0.01). ns, no significant difference. (g) GUS activity analysis showing that phosphorylated MdERF5 enhances its inhibitory activity. The MdERF5, MdERF5^{S260A} or MdERF5^{S260D} effector vector and the reporter vector containing the *MdACS1* promoter were infiltrated into tobacco leaves to analyze the regulation of GUS activity. S260A, Ser260 to Ala (phosphodeficient form); S260D, Ser260 to Asp (phosphomimetic form). Values represent means ± SE. Each dot represents a biologically independent sample. Asterisks indicate significantly different values (**, *P* < 0.01; *, *P* < 0.05).

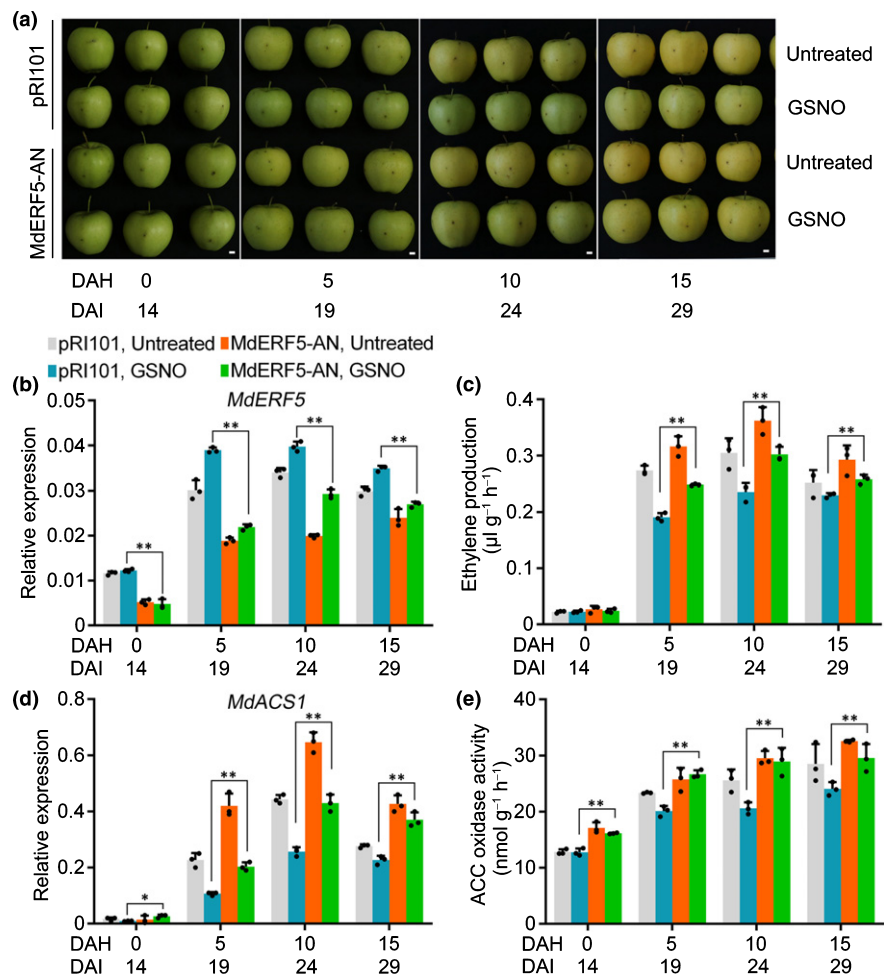


Fig. 9 *MdERF5* is involved in nitric oxide (NO)-suppressed ethylene biosynthesis in apple fruit (ERF, ETHYLENE RESPONSE FACTOR). *MdERF5* was silenced in apple fruit (MdERF5-AN) using *Agrobacterium tumefaciens*-mediated transient transformation. Fruit infiltrated with an empty pRI101 vector were used as controls (pRI101). MdERF5-AN and control fruits were harvested 14 d after infiltration, immediately treated with S-nitrosoglutathione (GSNO) and then stored at room temperature for 15 d (a). *MdERF5* expression was examined by quantitative real-time (qRT)-PCR (b). Ethylene production (c), 1-aminocyclopropane-1-carboxylic acid (ACC) synthase *MdACS1* expression (d), and ACC oxidase (ACO) enzyme activity (e) were investigated. Untreated, fruit not receiving any treatment; GSNO, fruit treated with GSNO; DAH, days after harvest; DAI, days post-infiltration. For qRT-PCR, three biological replicates were analyzed as described in the Materials and Methods section. Values represent means ± SE. Each dot represents a biologically independent sample. Statistical significance was determined using a Student's *t*-test (**, *P* < 0.01; *, *P* < 0.05).

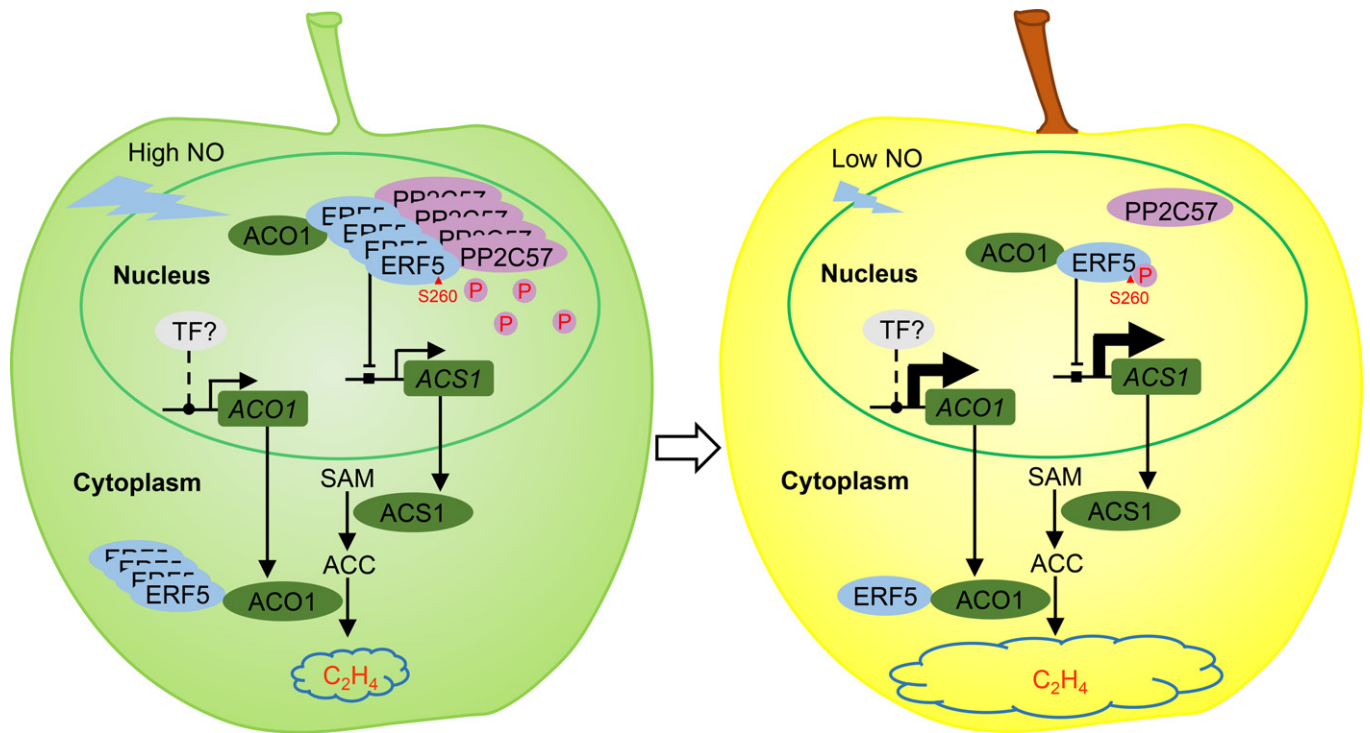


Fig. 10 Model showing the regulation by nitric oxide (NO) on apple ethylene biosynthesis. When endogenous NO content is high, ETHYLENE RESPONSE FACTOR *MdERF5* expression is enhanced and *MdERF5* that has been dephosphorylated by protein phosphatase *MdPP2C57* moves into the cytoplasm. *MdERF5* in the cytoplasm suppresses ACC oxidase 1 (ACO1) enzyme activity by direct protein interaction. *MdERF5* localized in the nucleus suppresses the transcription of the ethylene biosynthetic ACC synthase gene *MdACS1* by direct promoter binding, thereby suppressing ethylene biosynthesis. When endogenous NO content decreases, *MdERF5* expression declines and most of the *MdERF5* is retained in the nucleus, which weakens the suppression by *MdERF5* of *MdACO1* enzyme activity and *MdACS1* transcription, leading to a burst in ethylene production and fruit ripening. →, promotion; ⊥, suppression; ■, ERF-binding site; ●, other transcription factor (TF) binding site; SAM, S-adenosyl methionine; ACC, 1-aminocyclopropane-1-carboxylic acid; C₂H₄, ethylene.

among many fruit crops, including apple (Shaw *et al.*, 1996), tomato (Zhang *et al.*, 1997), avocado (*Persea americana*) (Rocklin *et al.*, 1999) and pear (Ji *et al.*, 2021), and substitutions of Fe (II) binding site residues H177, D179 and H234 by site-directed mutagenesis result in a complete loss of ACO activity (Fig. S15). In our study, we observed that *MdERF5* interacted with the *MdACO1D* fragment, which contains the three Fe(II) binding sites (Figs 7f, S15). We concluded that NO-enhanced *MdERF5*–*MdACO1* interaction might block Fe(II) from binding to *MdACO1*, thereby suppressing *MdACO1* activity and ethylene biosynthesis.

In addition, we found that *MdERF5* binds to the *MdACS1* promoter to directly downregulate its expression (Fig. 8). ACS is the central rate-limiting enzyme in ethylene biosynthesis (Gupta *et al.*, 2013), and its promoter has the DRE motif to which ERF TFs bind. Yeast-one-hybrid (Y1H), electrophoretic mobility shift assay (EMSA) and chromatin immunoprecipitation (ChIP)-PCR assays all showed that *MdERF5* binds to the dehydration-related element (DRE) motif in the *MdACS1* promoter (Figs 8a–c, S17b). We observed that *MdERF5* directly suppressed *MdACS1* transcription and that GSNO treatment strengthened this suppression in β-glucuronidase (GUS) transactivation analysis (Fig. 8d). In addition, we found that *MdERF5* protein levels

gradually increased in the cytoplasm during storage (Fig. 3e). This suggests that the accumulation of cytosolic *MdERF5* suppresses *MdACO1* enzyme activity by interacting with *MdACO1*. A notable finding in our study was that the GSNO treatment also promoted the nuclear accumulation of *MdERF5* (Fig. 3d), indicating that the accumulation of nuclear *MdERF5* suppresses *MdACS1* expression mediated by NO.

ACO is the other key rate-limiting enzyme in ethylene biosynthesis (Schaffer *et al.*, 2007), and GSNO treatment was found to suppress *MdACO1* expression (Fig. 1g). However, the *MdACO1* promoter does not contain a putative DRE motif or GCC-box, and the *MdACO1* expression levels were similar in *MdERF5*-AN calli than in control calli (Fig. S4), implying that other TFs inhibit the expression of *MdACO1* during NO-suppressed ethylene biosynthesis.

Dephosphorylation of *MdERF5* enables it to act as a nucleocytoplasmic shuttling protein

Nucleocytoplasmic protein shuttling is integral to the transmission of signals between the nucleus and the cytoplasm in plants and mammals (Ryu *et al.*, 2007; Jordan & Kreutz, 2009; Ju *et al.*, 2012; Zhang *et al.*, 2019). There is increasing evidence that

nucleocytoplasmic protein shuttling is related to protein phosphorylation and dephosphorylation. For example, brassinazole resistant 1 (BZR1) functions as a nucleocytoplasmic shuttling protein and glycogen synthase kinase-3 (GSK3)-like kinases induce the nuclear export of BZR1 by modulating BZR1 interaction with the 14-3-3 proteins (Ryu *et al.*, 2007). The nuclear accumulation of membrane-tethered myeloblastosis protein RhPTM mediated by phosphorylation of a plasma membrane intrinsic protein (PIP)-type aquaporin regulates a trade-off mechanism between plant growth and survival under water-deficiency conditions in rose (*Rosa hybrida*) (Zhang *et al.*, 2019). However, we are not aware of any reports to date of ERF proteins shuttling between the nucleus and cytoplasm.

Here, we identified *MdERF5* from apple and found that it shuttles between the nucleus and the cytoplasm in a process that is mediated by NO (Figs 3a,b, S5). We observed that MdERF5 protein levels gradually increased in the cytoplasm and that NO promoted the accumulation of MdERF5 protein in the cytoplasm during storage (Fig. 3e). The nucleocytoplasmic shuttling of MdERF5 represents a newly revealed bridge linking the NO and ethylene signals, and has important physiological significance for regulating ethylene biosynthesis in apple.

Previous studies have shown that protein expression, structure, stability and subcellular localization are regulated by post-translational modifications (PTMs) such as phosphorylation, acetylation, methylation and glycosylation (Ryu *et al.*, 2007; Zhang *et al.*, 2019). Phosphorylation is the most common PTM and is involved in essentially all cellular and extracellular processes, such as defense responses, signal transduction and apoptosis (Benschop *et al.*, 2007; Nakagami *et al.*, 2010). We found that MdERF5 is highly phosphorylated but is rapidly dephosphorylated in response to NO (Fig. 3f). Given that protein dephosphorylation often is regulated by protein phosphatase (PP) enzymes (Ryu *et al.*, 2007), we searched for and identified a PP2C gene, *MdPP2C57* and found that MdPP2C57 interacted with MdERF5 to dephosphorylate MdERF5 (Fig. 5a–c). We observed that overexpression of *MdPP2C57* resulted in translocation of MdERF5 to the plasma membrane (Fig. 5f), which was consistent with the subcellular distribution of MdERF5 in response to GSNO treatment (Fig. 3a). Moreover, the phosphomimetic form MdERF5^{S260D} only localized in the nucleus even under the overexpression of *MdPP2C57* (Fig. 6c). Accordingly, we propose that MdERF5 is a nucleocytoplasmic shuttling protein whose localization is tightly regulated by its phosphorylation status at Ser260, which in turn is determined by the PP2C-type phosphatase, MdPP2C57. In addition, there are some additional potential Ser/Thr phosphorylation sites in MdERF5, which also might influence the subcellular distribution of MdERF5.

MdERF5 functions in NO-suppressed ethylene biosynthesis

It is technically and experimentally challenging to generate transgenic apple fruit as a consequence of the long juvenile period (Kotoda *et al.*, 2006). Increasingly, researchers use a transient expression assay involving *A. tumefaciens* infiltration to study gene function in fruit (Ji *et al.*, 2021). We used this to transiently silence *MdERF5* expression in apple fruit to

confirm the role of MdERF5 in NO-suppressed ethylene biosynthesis. *MdERF5*-suppressed apple fruit showed faster ripening than control fruit after GSNO treatment (Figs 9a, S20a), as well as significantly higher ethylene production (Figs 9c, S20c), *MdACS1* expression and MdACO1 enzyme activity (Figs 9d,e, S20d,e). These results support the conclusion that NO suppresses ethylene biosynthesis in apple fruit through regulating MdERF5 activity, which in turn regulates the expression of ethylene biosynthetic genes and ACO enzyme activity.

Having been first characterized as a specific diffusible molecular messenger in animals, NO was hypothesized to produce similar signal transductions in plants. Although the enzymatic NO source L-arginine-dependent nitric oxide synthase (NOS) has been well-characterized in mammalian systems, identification of NOS has not been performed in plants currently. Furthermore, knowledge of NO generation in higher plants remains limited (Corpas *et al.*, 2022), including apple. However, previous studies have documented that NO regulates multiple transcription factors involved in the regulatory mechanisms of plant growth and development. For example, NO regulates *ABA-Insensitive 5 (ABI5)* transcription through controlling ERF stability (Gibbs *et al.*, 2014) and NO triggers the ABI5 degradation by S-nitrosylation to promote seed germination and seedling growth (Albertos *et al.*, 2015). NO accumulation promotes zinc finger protein *SRG1* and *SRG3* expression and triggers the S-nitrosylation of SRG1 and SRG3 to regulate plant immunity (Cui *et al.*, 2018, 2021). In this work, we observed that *MdERF5* expression is activated by NO in apple fruit, but the underlying mechanism remains unclear. It is possible that the TF(s) in NO signal transduction, which has(have) not yet been identified, might regulate the *MdERF5* expression. Also, it cannot be excluded that NO recruits acetyltransferase to indirectly regulate the *MdERF5* expression. The mechanistic basis of the upregulated *MdERF5* by NO will be an interesting research direction in the future.

A model of how NO regulates ethylene biosynthesis in climacteric fruit is shown in Fig. 10. When endogenous NO content is high, *MdERF5* expression is enhanced and the MdERF5 protein, which is dephosphorylated at Ser260 by protein phosphatase MdPP2C57, moves into the cytoplasm, where it suppresses MdACO1 enzyme activity in the cytoplasm via a direct protein interaction. The nucleus-retained MdERF5 suppresses the transcription of the ethylene biosynthetic gene *MdACS1* in the nucleus by direct promoter binding and so ethylene biosynthesis is limited. When endogenous NO content is low, *MdERF5* expression declines and most MdERF5 is retained in the nucleus, which weakens the MdERF5-mediated suppression of MdACO1 enzyme activity and *MdACS1* transcription, leading to a burst in ethylene production and fruit ripening.

Accession numbers

Sequence data from this article can be found in the Genome Database for Rosaceae (<https://www.rosaceae.org>) or GenBank libraries under accession nos. MdERF5 (XM008365562), *MdACS1* (U89156), *MdACO1* (AF030859), *MdPP2C57* (XM008378526), *MdActin* (EB136338).




Acknowledgements

This work was supported by the National Natural Science Foundation of China (31972376, 32125034), and the National Key Research and Development Program of China (2018YFD1000105). We thank PlantScribe (<http://www.plantscribe.com>) for editing this manuscript.

Author contributions

AW and YJ conceived and designed this research; YJ and MX performed most of the experiments; ZL and TL provided the plant materials; HY performed the library screening; YS, HL and YX performed protein purification; and AW and YJ wrote the article. All authors analyzed the data and discussed the article.

ORCID

Yinglin Ji  <https://orcid.org/0000-0002-1595-1998>
Aide Wang  <https://orcid.org/0000-0002-7034-7021>
Hui Yuan  <https://orcid.org/0000-0002-4935-3988>

Data availability

The data that support the findings of this study are available from the corresponding author upon request. Data generated during the study were deposited in the NCBI under accession no. PRJNA658005.

References

- Albertos P, Romero-Puertas MC, Tatematsu K, Mateos I, Sanchez-Vicente I, Nambara E, Lorenzo O. 2015. S-nitrosylation triggers ABI5 degradation to promote seed germination and seedling growth. *Nature Communications* 6: 8669.
- Beligni MV, Lamattina L. 2000. Nitric oxide stimulates seed germination and de-etiolation, and inhibits hypocotyl elongation, three light-inducible responses in plants. *Planta* 210: 215–221.
- Benschop JJ, Mohammed S, O'Flaherty M, Heck AJ, Slijper M, Menke FL. 2007. Quantitative phosphoproteomics of early elicitor signaling in Arabidopsis. *Molecular & Cellular Proteomics* 6: 1198–1214.
- Besson-Bard A, Pugin A, Wendehenne D. 2008. New insights into nitric oxide signaling in plants. *Annual Review of Plant Biology* 59: 21–39.
- Bodanapu R, Gupta SK, Basha PO, Sakthivel K, Sadhana, Sreelakshmi Y, Sharma R. 2016. Nitric oxide overproduction in tomato shr mutant shifts metabolic profiles and suppresses fruit growth and ripening. *Frontiers in Plant Science* 7: 1714.
- Bowyer MC, Wills RBH, Badiyan D, Ku VVV. 2003. Extending the postharvest life of carnations with nitric oxide—comparison of fumigation and *in vivo* delivery. *Postharvest Biology and Technology* 30: 281–286.
- Cheng G, Yang E, Lu W, Jia Y, Jiang Y, Duan X. 2009. Effect of nitric oxide on ethylene synthesis and softening of banana fruit slice during ripening. *Journal of Agricultural and Food Chemistry* 57: 5799–5804.
- Corpas FJ, Gonzalez-Gordo S, Palma JM. 2020. Nitric oxide: a radical molecule with potential biotechnological applications in fruit ripening. *Journal of Biotechnology* 324: 211–219.
- Corpas FJ, Gonzalez-Gordo S, Palma JM. 2022. NO source in higher plants: present and future of an unresolved question. *Trends in Plant Science* 27: 116–119.
- Correa-Aragunde N, Graziano M, Lamattina L. 2004. Nitric oxide plays a central role in determining lateral root development in tomato. *Planta* 218: 900–905.
- Cui B, Pan Q, Clarke D, Villarreal MO, Umbreen S, Yuan B, Shan W, Jiang J, Loake GJ. 2018. S-nitrosylation of the zinc finger protein SRG1 regulates plant immunity. *Nature Communications* 9: 4226.
- Cui B, Xu S, Li Y, Umbreen S, Frederickson D, Yuan B, Jiang J, Liu F, Pan Q, Loake GJ. 2021. The Arabidopsis zinc finger proteins SRG2 and SRG3 are positive regulators of plant immunity and are differentially regulated by nitric oxide. *New Phytologist* 230: 259–274.
- Dandekar AM, Teo G, Defilippi BG, Uratsu SL, Passey AJ, Kader AA, Stow JR, Colgan RJ, James DJ. 2004. Effect of down-regulation of ethylene biosynthesis on fruit flavor complex in apple fruit. *Transgenic Research* 13: 373–384.
- Dong JG, Fernandez-Maculet JC, Yang SF. 1992. Purification and characterization of 1-aminocyclopropane-1-carboxylate oxidase from apple fruit. *Proceedings of the National Academy of Sciences, USA* 89: 9789–9793.
- Duan X, Su X, You Y, Qu H, Li Y, Jiang Y. 2007. Effect of nitric oxide on pericarp browning of harvested longan fruit in relation to phenolic metabolism. *Food Chemistry* 104: 571–576.
- Ederli L, Morettini R, Borgogni A, Wasternack C, Miersch O, Reale L, Ferranti F, Tosti N, Pasqualini S. 2006. Interaction between nitric oxide and ethylene in the induction of alternative oxidase in ozone-treated tobacco plants. *Plant Physiology* 142: 595–608.
- Eum HL, Kim HB, Choi SB, Lee SK. 2008. Regulation of ethylene biosynthesis by nitric oxide in tomato (*Solanum lycopersicum* L.) fruit harvested at different ripening stages. *European Food Research and Technology* 228: 331–338.
- Fan S, Meng Y, Song M, Pang C, Wei H, Liu JI, Zhan X, Lan J, Feng C, Zhang S *et al.* 2014. Quantitative phosphoproteomics analysis of nitric oxide-responsive phosphoproteins in cotton leaf. *PLoS ONE* 9: e94261.
- Feechan A, Kwon E, Yun B-W, Wang Y, Pallas JA, Loake GJ. 2005. A central role for S-nitrosothiols in plant disease resistance. *Proceedings of the National Academy of Sciences, USA* 102: 8054–8059.
- Fenn MA, Giovannoni JJ. 2021. Phytohormones in fruit development and maturation. *The Plant Journal* 105: 446–458.
- Gibbs D, Md Isa N, Movahedi M, Lozano-Juste J, Mendiondo G, Berckhan S, Marín-de la Rosa N, Vicente Conde J, Sousa Correia C, Pearce SP *et al.* 2014. Nitric oxide sensing in plants is mediated by proteolytic control of group VII ERF transcription factors. *Molecular Cell* 53: 369–379.
- Gupta A, Pal RK, Rajam MV. 2013. Delayed ripening and improved fruit processing quality in tomato by RNAi-mediated silencing of three homologs of 1-aminocyclopropane-1-carboxylate synthase gene. *Journal of Plant Physiology* 170: 987–995.
- He Y, Tang R-H, Hao Y, Stevens RD, Cook CW, Ahn SM, Jing L, Yang Z, Chen L, Guo F. 2004. Nitric oxide represses the Arabidopsis floral transition. *Science* 305: 1968–1971.
- Huang G, Li T, Li X, Tan D, Jiang Z, Wei Y, Li J, Wang A. 2014. Comparative transcriptome analysis of climacteric fruit of Chinese pear (*Pyrus ussuriensis*) reveals new insights into fruit ripening. *PLoS ONE* 9: e107562.
- Ji Y, Qu Y, Jiang Z, Yan J, Chu J, Xu M, Su X, Yuan H, Wang A. 2021. The mechanism for brassinosteroids suppressing climacteric fruit ripening. *Plant Physiology* 185: 1875–1893.
- Jordan BA, Kreutz MR. 2009. Nucleocytoplasmic protein shuttling: the direct route in synapse-to-nucleus signaling. *Trends in Neurosciences* 32: 392–401.
- Ju C, Yoon GM, Shemansky JM, Lin DY, Ying ZI, Chang J, Garrett WM, Kessenbrock M, Groth G, Tucker ML. 2012. CTR1 phosphorylates the central regulator EIN2 to control ethylene hormone signaling from the ER membrane to the nucleus in Arabidopsis. *Proceedings of the National Academy of Sciences, USA* 109: 19486–19491.
- Kolbert Z, Feigl G, Freschi L, Poor P. 2019. Gasotransmitters in action: nitric oxide-ethylene crosstalk during plant growth and abiotic stress responses. *Antioxidants* 8: 167–189.
- Kotoda N, Iwanami H, Takahashi S, Abe K. 2006. Antisense expression of MdTFL1, a TFL1-like gene, reduces the juvenile phase in apple. *Journal of the American Society for Horticultural Science* 131: 74–81.
- Lee U, Wie C, Fernandez BO, Feelisch M, Vierling E. 2008. Modulation of nitrosative stress by S-nitrosoglutathione reduction is critical for thermotolerance and plant growth in Arabidopsis. *Plant Cell* 20: 786–802.
- Leshem YY, Wills RBH. 1998. Harnessing senescence delaying gases nitric oxide and nitrous oxide: a novel approach to postharvest control of fresh horticultural produce. *Biologia Plantarum* 41: 1–10.

- Li T, Jiang Z, Zhang L, Tan D, Wei Y, Yuan H, Li T, Wang A. 2016. Apple (*Malus domestica*) MdERF2 negatively affects ethylene biosynthesis during fruit ripening by suppressing MdACS1 transcription. *The Plant Journal* 88: 735–748.
- Li T, Li X, Tan D, Jiang Z, Wei Y, Li J, Du G, Wang A. 2014. Distinct expression profiles of ripening related genes in the 'Nanguo' pear (*Pyrus ussuriensis*) fruits. *Scientia Horticulturae* 171: 78–82.
- Li T, Tan D, Liu Z, Jiang Z, Wei Y, Zhang L, Li X, Yuan H, Wang A. 2015. Apple MdACS6 regulates ethylene biosynthesis during fruit development involving ethylene-responsive factor. *Plant & Cell Physiology* 56: 1909–1917.
- Li T, Xu Y, Zhang L, Ji Y, Tan D, Yuan H, Wang A. 2017. The jasmonate-activated transcription factor MdMYC2 regulates ETHYLENE RESPONSE FACTOR and ethylene biosynthetic genes to promote ethylene biosynthesis during apple fruit ripening. *Plant Cell* 29: 1316–1334.
- Lin Z, Zhong S, Grierson D. 2009. Recent advances in ethylene research. *Journal of Experimental Botany* 60: 3311–3336.
- Lindermayr C, Saalbach G, Bahnweg G, Durner J. 2006. Differential inhibition of Arabidopsis methionine adenosyltransferases by protein S-nitrosylation. *Journal of Experimental Botany* 281: 4285–4291.
- Meng X, Xu J, He Y, Yang KY, Mordorski B, Liu Y, Zhang S. 2013. Phosphorylation of an ERF transcription factor by Arabidopsis MPK3/MPK6 regulates plant defense gene induction and fungal resistance. *Plant Cell* 25: 1126–1142.
- Mur LA, Mandon J, Persijn S, Cristescu SM, Moshkov IE, Novikova GV, Hall MA, Harren FJ, Hebelstrup KH, Gupta KJ. 2013. Nitric oxide in plants: an assessment of the current state of knowledge. *AoB Plants* 5: pls052.
- Nakagami H, Sugiyama N, Mochida K, Daudi A, Yoshida Y, Toyoda T, Tomita M, Ishihama Y, Shirasu K. 2010. Large-scale comparative phosphoproteomics identifies conserved phosphorylation sites in plants. *Plant Physiology* 153: 1161–1174.
- Otvos K, Pasternak TP, Miskolczi P, Domoki M, Dorjgotov D, Szucs A, Bottka S, Dudits D, Feher A. 2005. Nitric oxide is required for, and promotes auxin-mediated activation of, cell division and embryonic cell formation but does not influence cell cycle progression in alfalfa cell cultures. *The Plant Journal* 43: 849–860.
- Palma JM, Freschi L, Rodriguez-Ruiz M, Gonzalez-Gordo S, Corpas FJ. 2019. Nitric oxide in the physiology and quality of fleshy fruits. *Journal of Experimental Botany* 70: 4405–4417.
- Prado AM, Porterfield DM, Feijo JA. 2004. Nitric oxide is involved in growth regulation and re-orientation of pollen tubes. *Development* 131: 2707–2714.
- Rocklin AM, Tierney DL, Kofman V, Brunhuber NM, Hoffman BM, Christoffersen RE, Reich NO, Lipscomb JD, Que L. 1999. Role of the nonheme Fe (II) center in the biosynthesis of the plant hormone ethylene. *Proceedings of the National Academy of Sciences, USA* 96: 7905–7909.
- Rudell DR, Mattheis JP. 2006. Nitric oxide and nitrite treatments reduce ethylene evolution from apple fruit disks. *HortScience* 41: 1462–1465.
- Ryu H, Kim K, Cho H, Park J, Choe S, Hwang I. 2007. Nucleocytoplasmic shuttling of BZR1 mediated by phosphorylation is essential in Arabidopsis brassinosteroid signaling. *Plant Cell* 19: 2749–2762.
- Schaffer RJ, Friel EN, Souleyre EJ, Bolitho K, Thodey K, Ledger S, Bowen JH, Ma J-H, Nain B, Cohen D. 2007. A genomics approach reveals that aroma production in apple is controlled by ethylene predominantly at the final step in each biosynthetic pathway. *Plant Physiology and Biochemistry* 144: 1899–1912.
- Shaw J-F, Chou Y-S, Chang R-C, Yang SF. 1996. Characterization of the ferrous ion binding sites of apple 1-aminocyclopropane-1-carboxylate oxidase by site-directed mutagenesis. *Biochemical and Biophysical Research Communications* 225: 697–700.
- Tada Y, Spoel SH, Pajeroska-Mukhtar K, Mou Z, Song J, Wang C, Zuo J, Dong X. 2008. Plant immunity requires conformational changes of NPR1 via S-nitrosylation and thioredoxins. *Science* 321: 952–956.
- Umezawa T, Sugiyama N, Mizoguchi M, Hayashi S, Myouga F, Yamaguchi-Shinozaki K, Ishihama Y, Hirayama T, Shinozaki K. 2009. Type 2C protein phosphatases directly regulate abscisic acid-activated protein kinases in Arabidopsis. *Proceedings of the National Academy of Sciences, USA* 106: 17588–17593.
- Walter M, Chaban C, Schütze K, Batistic O, Weckermann K, Nägele C, Blazevic D, Grefen C, Schumacher K, Oecking C *et al.* 2004. Visualization of protein interactions in living plant cells using bimolecular fluorescence complementation. *The Plant Journal* 40: 428–438.
- Wilhelmova H, Fuksova M, Srbova D, Mikov Z, Mytinova D, Prochazkova R, Vytsek JW. 2006. The effect of plant cytokinin hormones on the production of ethylene, nitric oxide, and protein nitrotyrosine in ageing tobacco leaves. *BioFactors* 27: 203–211.
- Wills R, Ku V, Leshem Y. 2000. Fumigation with nitric oxide to extend the postharvest life of strawberries. *Postharvest Biology and Technology* 18: 75–79.
- Xiao YY, Chen JY, Kuang JF, Shan W, Xie H, Jiang YM, Lu WJ. 2013. Banana ethylene response factors are involved in fruit ripening through their interactions with ethylene biosynthesis genes. *Journal of Experimental Botany* 64: 2499–2510.
- Ya'Acov YL, Haramaty E. 1996. The characterization and contrasting effects of the nitric oxide free radical in vegetative stress and senescence of *Pisum sativum* Linn. foliage. *Journal of Plant Physiology* 148: 258–263.
- Ya'Acov YL, Wills RB, Ku VV-V. 1998. Evidence for the function of the free radical gas—nitric oxide (NO[•])—as an endogenous maturation and senescence regulating factor in higher plants. *Plant Physiology and Biochemistry* 36: 825–833.
- Yang SF, Hoffman NE. 1984. Ethylene biosynthesis and its regulation in higher plants. *Annual Review of Plant Physiology and Plant Molecular Biology* 35: 155–189.
- Yoo S-D, Cho Y-H, Sheen J. 2007. Arabidopsis mesophyll protoplasts: a versatile cell system for transient gene expression analysis. *Nature Protocols* 2: 1565–1572.
- Yu M, Lamattina L, Spoel SH, Loake GJ. 2014. Nitric oxide function in plant biology: a redox cue in deconvolution. *New Phytologist* 202: 1142–1156.
- Zhang S, Feng M, Chen W, Zhou X, Lu J, Wang Y, Li Y, Jiang C-Z, Gan S-S, Ma N *et al.* 2019. In rose, transcription factor PTM balances growth and drought survival via PIP2; 1 aquaporin. *Nature Plants* 5: 290–299.
- Zhang Z, Barlow JN, Baldwin JE, Schofield CJ. 1997. Metal-catalyzed oxidation and mutagenesis studies on the iron (II) binding site of 1-aminocyclopropane-1-carboxylate oxidase. *Biochemistry* 36: 15999–16007.
- Zhu S, Liu M, Zhou J. 2006. Inhibition by nitric oxide of ethylene biosynthesis and lipoxygenase activity in peach fruit during storage. *Postharvest Biology and Technology* 42: 41–48.
- Zuccarelli R, Rodriguez-Ruiz M, Lopes-Oliveira PJ, Pascoal GB, Andrade SCS, Furlan CM, Purgatto E, Palma JM, Corpas FJ, Rossi M *et al.* 2020. Multifaceted roles of nitric oxide in tomato fruit ripening: NO-induced metabolic rewiring and consequences for fruit quality traits. *Journal of Experimental Botany* 72: 941–958.

Supporting Information

Additional Supporting Information may be found online in the Supporting Information section at the end of the article.

Fig. S1 Ethylene production, fruit firmness and NO content in apple fruit treated with GSNO and sodium nitroprusside.

Fig. S2 Ethylene production, fruit firmness, nitric oxide content and gene expression in apple fruit treated with GSNO.

Fig. S3 *MdERF5* gene expression in apple fruit.

Fig. S4 *MdACO1* gene expression in *MdERF5*-silenced calli.

Fig. S5 Subcellular localization of *MdERF5* with SNP treatment.

Fig. S6 Original figure of *MdERF5* phosphorylation suppressed by GSNO treatment.

Fig. S7 Subcellular localization of MdERF5 treated with GSNO and okadaic acid.

Fig. S8 MdPP2C57 interacts with MdERF5N/D in yeast cells.

Fig. S9 Subcellular co-localization of MdPP2C57 and MdERF5.

Fig. S10 MdPP2C57 mediates the nucleocytoplasmic shuttling of MdERF5.

Fig. S11 Nuclear localization signal prediction of MdERF5.

Fig. S12 Subcellular localization of MdACO1.

Fig. S13 Subcellular co-localization of MdACO1 and MdERF5.

Fig. S14 Nitric oxide enhances the MdERF5-MdACO1 interaction.

Fig. S15 MdACO1 protein domain model.

Fig. S16 ACO activity in apple fruit.

Fig. S17 Binding of MdERF5 to the *MdACS1* promoter.

Fig. S18 *MdERF5* was overexpressed in apple fruit calli.

Fig. S19 MdERF5–MdACO1 interaction does not affect the binding of MdERF5 to the *MdACS1* promoter.

Fig. S20 *MdERF5* is involved in NO-suppressed ethylene biosynthesis in apple fruit.

Methods S1 Quantification of endogenous NO content.

Methods S2 Y2H assay.

Methods S3 Co-IP assay.

Methods S4 Firefly Luc complementation imaging assay.

Methods S5 Measurements of ACO activity.

Methods S6 GUS analysis.

Methods S7 *Agrobacterium tumefaciens* infiltration.

Tables S1 Primers used in this study.

Table S2 Differentially expressed genes identified from RNA-seq data derived from untreated apple fruit and fruit treated with GSNO.

Table S3 NO-regulated *ERF* identified from RNA-seq data derived from untreated apple fruit and fruit treated with GSNO.

Table S4 NO-regulated *PP2C* identified from RNA-seq data derived from untreated apple fruit and fruit treated with GSNO.

Please note: Wiley Blackwell are not responsible for the content or functionality of any Supporting Information supplied by the authors. Any queries (other than missing material) should be directed to the *New Phytologist* Central Office.